# The Effect of Cut-out Hole Size on the Formability of Hole Flanging by Multistage Incremental Forming

**Hatef Valaei**

Submitted to the
Institute of Graduate Studies and Research
in partial fulfillment of the requirements for the Degree of

Master of Science
in
Mechanical Engineering

Eastern Mediterranean University
July 2014
Gazimağusa, North Cyprus

Approval of the Institute of Graduate Studies and Research

Prof. Dr. Elvan Yılmaz
Director

I certify that this thesis satisfies the requirements as a thesis for the degree of Master of Science in Mechanical Engineering.

Prof. Dr. Uğur Atikol
Chair, Department of Mechanical Engineering

We certify that we have read this thesis and that in our opinion it is fully adequate in scope and quality as a thesis for the degree of Master of Science in Mechanical Engineering.

Asst. Prof. Dr. Ghulam Hussain
Supervisor

Examining Committee

1. Assoc. Prof. Dr. Hasan Hacışevki
2. Asst. Prof. Dr. Ghulam Hussain
3. Dr. Kiyan Parham

# ABSTRACT

Single point incremental forming is advancing to replace the conventional sheet forming processes. Multi stage incremental forming is introduced to cover some shortcomings of this process and extend the complexity of the shapes that cannot be produced in single stage incremental forming. This method does not require any special equipment and is very economic.

In this study the effect of varying cut-out hole size on the formability of hole flanging in multi-stage incremental forming and on the thickness distribution of flange is investigated. The AA1060 aluminum is taken as the experimental material, and the formability is measured as the flange depth without sheet fracture. The flanges are made in 4 stages of 45°, 60°, 75° and 90° at room temperature. Furthermore, the stress and strain patterns are studied utilizing ABAQUS software in order to understand the process mechanics.

The results have shown that the hole size has great effect on the flange depth and wall thickness of the part made by multistage incremental forming. The achieved depth decreases with increasing the hole size due to lack of material and thinning is less as the hole diameter gets larger.

The FEA results shows that increasing hole diameter will lead to lower stress and hoop strain levels due to decreasing the amount of material under load of the tool. Also it showed that a small amount of work hardening is useful for increasing the formability of the process.

**Keyword:** Multi stage incremental forming, formability, FEA ABAQUS, failure, hole flanging, hole diameter, stress level, strain level.

# ÖZ

Tek nokta artırımlı şekillendirme, konvansiyonel saç şekillendirme prosesinin yerini alma yönünde ilerlemektedir. Çok aşamalı atışlı şekillendirme metodu tek noktalı metodun eksikliklerini gidermek ve tek noktalı proses ile üretilemeyen kompleks parçaları üretmek için tanıtılmıştır. Bu metod herhangi özel bir ekipman gerektirmiyor ve çok ekonomiktir.

Bu çalışmada çok aşamalı atışlı şekillendirmenin delik ölçüsündeki değişikliklerin, delik flanş oluşumuna ve flanş kalınlığına etkisi incelenmiştir.
Deneysel malzeme olarak AA1060 aluminyum kullanılmış ve saç kırılması olmadan şekillendirme ve flanş derinliği ölçülmüştür . Flanşlar oda sıcaklığında 45° ,60°, 75° ve 90° olmak üzere dort aşamada yapılmıştır.

Prosesin mekaniğini anlamak için mukavemet hesapları ABAQUS yazılımı kullanılarak yapılmıştır. Çok aşamalı atışlı şekillendirme metodun delik ölçüsünün flanş derinliği ve et kalınlığı üzerinde büyük etkisi olduğu saptanmıştır. Elde edilen derinliğin delik ölçüsünün artması ile azaldığı, malzemenin kalınlığının azalması ve malzemenin kendisi ile alakalı olduğu ve incelmenin delik çapının artması ile azaldığı saptanmıştır.

**Anahtar kelime:** Çok aşamalı artışlı şekillendirme, şekillenebilirliği, FEA ABAQUS, şekillendirme başarısızlığı, flanş, delik çapı, stres düzeyi, gerginlik seviyesi.

# DEDICATION

**To My Family,**

**Romina and Findi**

# ACKNOWLEDGEMENT

I would like to thank Asst. Prof. Dr. Ghulam Hussain for his continuous support and guidance in the preparation of this study. Without his invaluable supervision, all my efforts could have been short-sighted.

Prof. Dr. Uğur Atikol, Chairman of the Department of Mechanical Engineering, Eastern Mediterranean University, helped me with various issues during the thesis and I am grateful to him. I am also obliged to Dr. Mehdi Shakoori Partovi for his help during my thesis. Besides, a number of friends had always been around to support me morally. I would like to thank them as well.

I owe quit a lot to my family who allowed me to travel all the way from Iran to Cyprus and supported me all throughout my studies. I would like to dedicate this study to them as an indication of their significance in this study as well as in my life.

# TABLE OF CONTENTS

# LIST OF TABLES

# LIST OF FIGURES

# LIST OF SYMBOLS/ABBRIVIATIONS

AL - Aluminum

CAD - Computer- Aided Design

CAM - Computer – Aided Manufacturing

CPU - Central Processing Unit

DOF - Degree of Freedom

FEA - Finite Element Analysis

FLD - Forming Limit Diagram

MK - Marciniak – Kuczynski

RPM - Rotation per minute

SPIF - Single Point Incremental Forming

ISF - Incremental sheet forming

TPIF - Two Point Incremental Forming

2D - Two Dimensional

3D - three Dimensional

**Greek Symbols**

Ø - Forming Angle

$Ø_{max}$ - Maximum Forming Angle

M - Coefficient of friction

α - Drawing Angle (Sine Law)

σ - Stress

ϵ - Strain

ϵt - Thickness Strain

$\epsilon_{\theta}$ - Hoop Strain

Є - Strain

Δz - Axial depth

$T_{f}$ - Final Thickness

$T_{o}$ - Original Thickness

n - Strain Hardening Coefficients

$A_{g}$ - Maximum Elongation

$A_{t}$ - Total Elongation

G - Shear Modulus

E - Modulus of Elasticity

V - Poisson's ratio

ρ - Mass Density

# Chapter 1

# INTRODUCTION

## 1.1 Conventional Sheet Metal Processes

Some of the most common conventional sheet metal forming processes are briefly introduced:

### 1.1.1 Hammering

Hammering is one of the oldest sheet metal forming processes which was conventionally done by hand. As the technology advances, nowadays this process is done by CNC machines and also in some cases robotic arms are used too. The process is consist of deforming a sheet which is clamped in a fixture with a tool controlled by computer or manually. The tool punches the sheet in circular motion and step down incrementally [1]. Schematics of this process are shown in Figure 1.1.

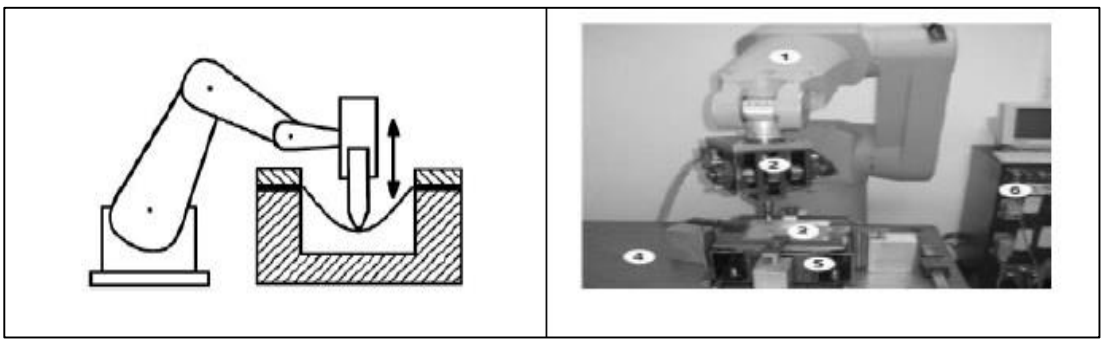

Figure 1.1: Hammering sheet forming process. (Left) incremental hammering (right) robotic arm used for hammering process [1].

### 1.1.2 Spinning

Spinning can be divided into two types:

*Conventional spinning and sheer spinning*

In conventional spinning the sheet is set on the mandrel of a lathe machine and the sheet is deformed using a roller or round tool. The deformation is taken place with imposing a localized stress on the sheet and deforming it in radial and axial directions. The production cost of this process is low and the process can be done manually or automatic. This process is suitable for small series of parts due to required very low number of steps for production.

Sheer spinning is also very similar to conventional spinning. The difference is the mechanism involved in deformation which in case of sheer spinning is stretching instead of bending in conventional spinning. Stretching will create material flow inside the sheet, so the thickness of the sheet will vary point by point. Sheer spinning is also called the ancestor of incremental sheet forming process [2].

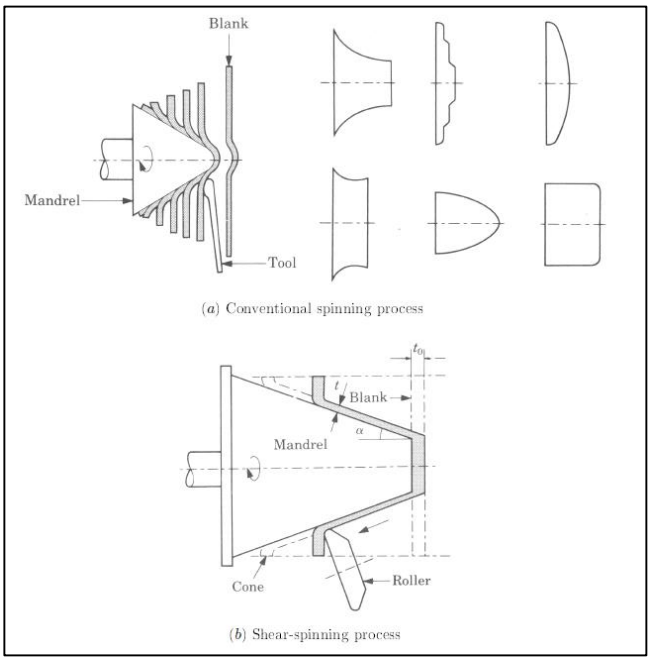


Figure 1.2: Schematics of conventional spinning and sheer spinning [2].

## 1.2 Background

During the past few years new demands of market caused to develop new methods of manufacturing. Incremental sheet forming is one the new forming methods that satisfies the demanded agility and flexibility of the market. A CNC machine, a spherical tool and a fixture is enough for this process which makes it to be categorized in low cost manufacturing methods for rapid prototyping and batch production so it can be used to form variety of sheets, symmetric and no symmetric, with wide range of thicknesses, a few microns to few millimeters. Some simple parts produced by this method are shown in figure 1.3.

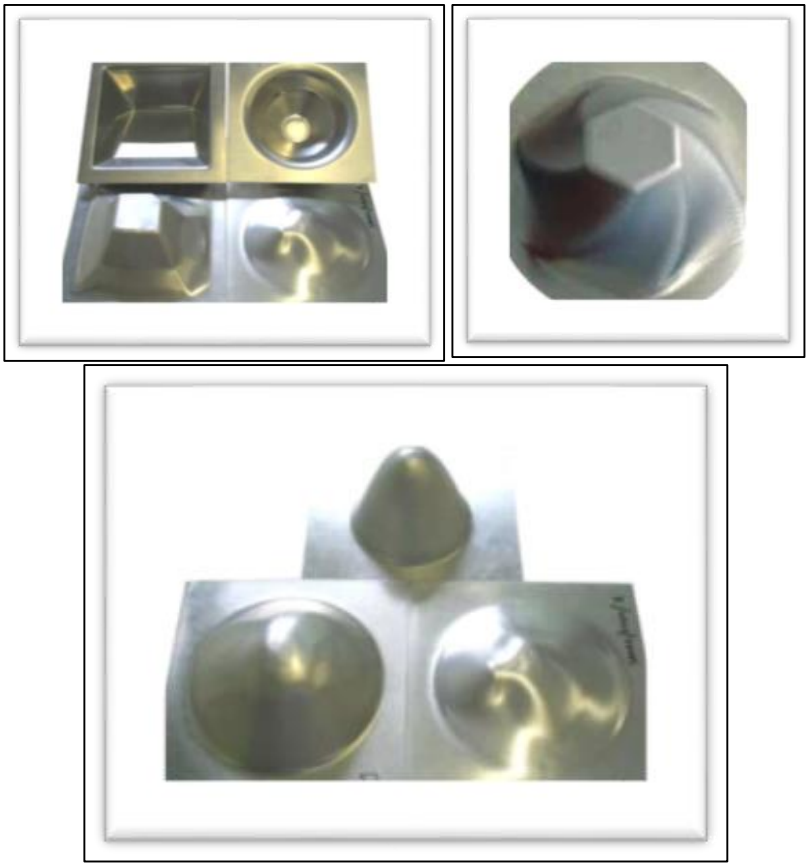

Figure 1.3: Simple parts made by ISF.

Main technologies that are used in ISF (incremental sheet forming) are introduced briefly regarding to figure 1.4:

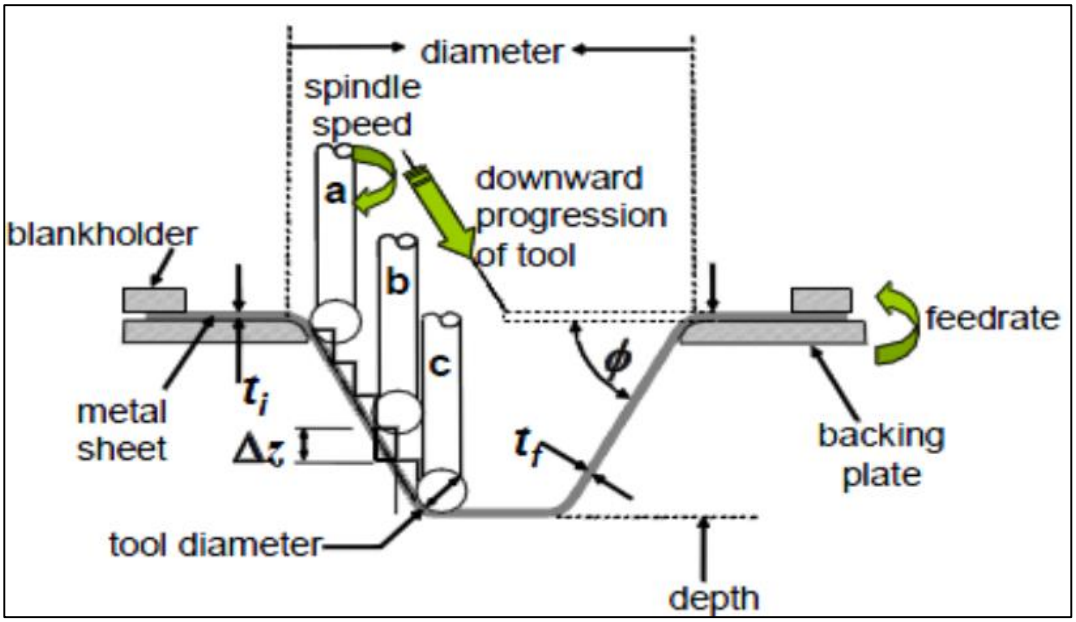


Figure 1.4: An illustration of ISF technology

ISf is a method of forming in which a tool with a spherical head moves along a path on the sheet and the deformation occurs towards it. The spherical head tool is clamped on the CNC machine, which gets the tool path from the cad software. Also a fixture system is applied to constrain the sheet and eliminate probable vibrations. As seen in the figure, $t_i$ is the initial sheet thickness that reduces to $t_f$ after deformation. $t_f$ Can vary point by point and is not constant throughout the sheet. Ø is the forming angle for the process and represents the inclined trend of the tool path and can be considered as a measure of material formability. The maximum angle (Ø max) is the greatest angle formed in a shape without any failures [3]. $\Delta z$ is the step size (also known as axial depth) that represents the amount of the step down after completing each contour.

## 1.3 Objective of Thesis

The aim of this thesis is to study the effect of the hole size diameter on different aspects of multi stage incremental forming or hole flanging like thickness distribution and depth. Then with utilizing FEA method the comparison will be taken place in order to verify the results and also with the help of FEA simulation some other parameters will be investigated like strains and stress levels.

## 1.4 Thesis Organization

This thesis in consist of 5 chapters. In the first chapter some basic information about incremental sheet forming process and the objective of the thesis is given. In chapter 2 a literature review is done about SPIF and multistage incremental forming process and the significant parameters influencing the process. The third chapter is about the experimental set up and material properties and organization of experiments. In the 4$^{th}$ chapter the FEA set up for ABAQUS is explained, how and why some preselected parameters are chosen will be discussed in this section such as Mesh type, mesh size, mass scaling and etc. The 5$^{th}$ chapter is to discuss the results and explain them. Also the suggestion for further study is mentioned in this chapter.

# Chapter 2

# LITERATURE REVIEW

## 2.1 Single point incremental forming

### 2.1.1 Process Definition

Incremental sheet forming has shown a great satisfaction to flexibility of manufactures part shapes and also to its diversity of use. Compared to other methods of sheet forming, ISF has less cost. Forming with this method needs a multi axis CNC machine, a spherical head tool. Unlike other methods of sheet forming such as drawing and stamping, ISF can produce both symmetric and no symmetric parts without using any die. This advantage can make this process very low cost method in comparison with other methods of sheet forming. However despite the advantage of low cost and easy setup which reduces the lead time, ISf has disadvantages like the time of process. The time of the process is higher than other techniques and it's only suitable for batch production. A simple fixture for ISF is shown in the figure 2.1:

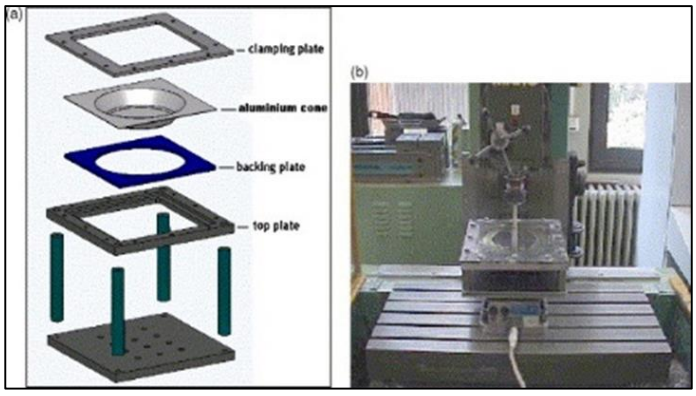

Figure 2.1: An illustration of Fixture used in SPIF [3]

The formable sheet is placed between two plates named clamping and back plate. Back plate can be changed according to the desired part diameter. On the clamping plate, there are some holes in which the screws are placed fastening the sheet on the back plate. The lower side of the rig is designed in a way that provides space for the deformed sheet and the tool when it goes down but the rods around this space or anything that is under the backing plate should be able to eliminate the vibrations and bear the forces during the process.

### 2.1.2 Significant Parameters

Some of the important factors that are involved in the incremental forming process are sheet thickness, tool path, forming tool, step size, lubrication, forming angle, tool feed rate and material used as sheet. Some of the parameters mentioned above will be discussed here.

### 2.1.3 Forming Tool

Tool diameter greatly effects the formability of the process. Small tool diameter tends to concentrate the stress on a small area which increases the total stress in result. It's obvious that the probability of failure in increased stress will be higher. But on the contrary some researches [6] show small tool diameters will provide better formability than the larger ones due to higher strains that impose to the sheet also larger tool diameters have greater contact area with the sheet but because of that the forces that imposes to sheet will be higher too. A simple spherical head tool is shown in the figure 2.2.

Figure 2.2: Simple forming tools used in SPIF [8]

Smaller tool diameters concentrates the stress and strain on the small area and provides higher formability. It is important that another consequence of this phenomena is temperature rising which itself provides a better forming condition for the sheet. This rising in temperature should be considered carefully when some specific materials such as plastics or PVC are being used.

### 2.1.4 Forming Tool Path

The deformation in ISF occurred because of moving the tool on the sheet along a specified path. This path is usually generated via the CAM software which is feed by the CAD model. Tool path has various models including step by step, helical and spiral form and etc. In general tool path has great effect on the formability of the process for example in order to decrease the stress concentration on the step down points, it's recommended to design the tool in a way that these points not get aligned on a line cause this will increase the probability of failure in the end of this step down line. Usually it is recommended to make these points aligned on helical line. Figure 2.3

shows a CAM software output of ISF tool path which is spiral to avoid step down points and lower roughness [7].

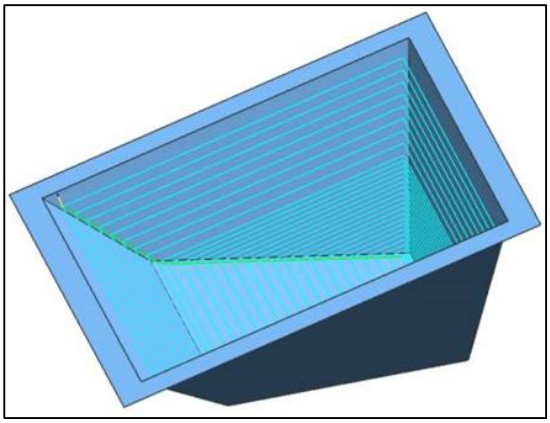

Figure 2.3: An illustration of tool path for SPIF.

### 2.1.5 Sheet Material

Different materials are used for ISF process. Each material will have its own formability which is influenced by other factors too. According to the research by Fratini et al [4] hardening exponent and also interaction of strength and strain hardening exponents have great effect on the formability of the materials used in ISF. Generally higher hardening exponent will lead to higher formability. However some considerations should be taken in account when using some specific type of materials like plastics and PVC which are very sensitive to temperature. During the ISF process a considerable amount of heat is generated, if the rise of temperature reaches a critical point during the process, the material been used can melt [4].

### 2.1.6 Forming Angle

Forming angle is the angle between the trend of the tool motion (or tool path) and the x-y plane of the initial flat sheet. This angle is strictly related to the material and the sheet thickness. Maximum forming angle (see figure 2.4) is a parameter specific for each material which is the angle that a material can be drawn before any failure occurs.

Previous research by martin gave an equation for maximum forming angle of a material by forming parameters [5].

$$\Phi = {}^{\pi}/_{2} - e^{\varepsilon t} \quad [9] \qquad \text{Eq.1.1}$$

In which t is the thickness of the sheet at the limit of formability and εt is the thickness strain. The equation represents the onset of fracture because it combines the ideas of both the fracture forming limit in principle strain space and the maximum forming angle at the onset of fracture [9].

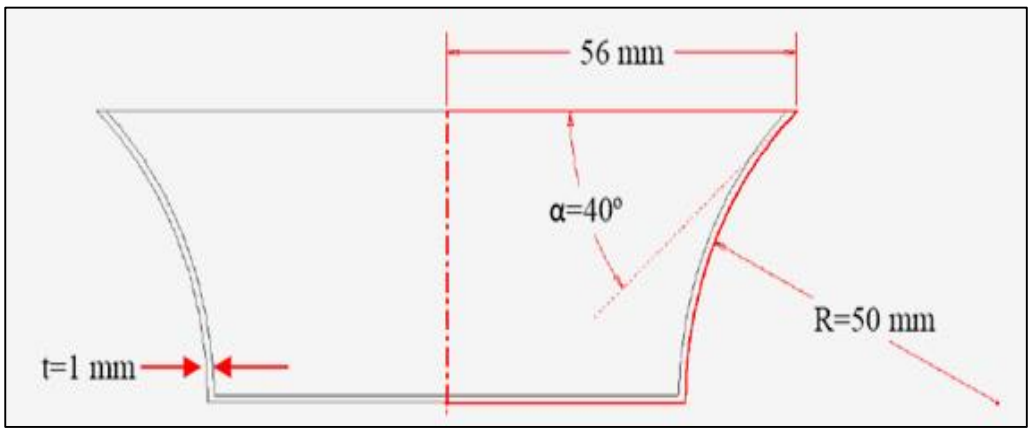

Figure 2.4: Maximum forming angle test for SPIF [13]

### 2.1.7 Step Size

Step size is the amount of tool motion along z-axis. As we decrease the step size, total time of the process increases due to increase in motions of the tool along z-axis. Some researcher's claim that the amount of step size does not effect in formability, on the contrary some other researchers talk about its significant role on formability, making this issue a debatable parameter in ISF. Recent research by Ham and Jeswiet shows that step size does not influence the formability of the material and has a great effect on the roughness of the sheet both inner side and outer side [8].

### 2.1.8 Forming Speed

Generally forming speeds can be divided into 2 sections which are spindle rotational speed and feed rate of the tool. Both are the major sources of the heat generated during the process because of the friction. It is claimed that higher forming speeds leads to higher formability due to increase in heat generating and rise in temperature which simplifies the forming process. But there are some defects that can be emerged by increasing the forming speed. High feed rates can make the surface roughness worse both inner side and outer side. And also higher tool wear rate and lubricant film breakdown can be other defects emerged here. Increasing forming speed will lead to rougher surface and lowering its quality also increasing the probability of surface waviness [9]. High rotational speed will also will increase the movement marks of the tool or tool chatter marks [10].

### 2.1.9 Lubrication

Lubrication is not widely investigated in case of SPIF. The only complements relating to lubrication is to reduce the friction, eliminate any possible material removal and improve surface quality. Also lower the heat generation rate caused by tool movement in case of temperature sensitive materials like plastics [11, 12].

## 2.2 Incremental Forming Types

Some types of incremental forming are developed in the last decades such as single point, two points, backward incremental forming and multistage incremental forming which will be discussed here.

### 2.2.1 Single Point Incremental Forming

Single Point Incremental Forming (SPIF) is a recently developed die less sheet metal part production technique that is gradually evolving towards industrial applicability. In this process a sheet metal part is formed in a stepwise fashion by a CNC controlled

rotating spherical tool without the need for a supporting (partial) die. This technique allows a relatively fast and cheap production of small series of sheet metal parts.

In the SPIF process generic, freeform shapes can be produced using a standard, spherical, CNC controlled tool. The process starts from a flat sheet metal blank, clamped on a sufficiently stiff rig and mounted on the table of a CNC machine. To form a part, the machine tool follows a pre-programmed contour, similar to a conventional milling operation. The main advantage of this method is that no die is required, making this an ideal process for rapid prototyping or small batch production. The first difference of the SPIF and other methods of incremental forming is that the tool is single providing only one contact point or contact area along the sheet [13]. Which TPIF that will be discussed later will provide two. Single point incremental forming is the conventional, most used and most researched type of ISF.

### 2.2.2 Two Point Incremental Forming

In SPIF no die is used. On the contrary in TPIF there is a die under the blank sheet which the desired shape will be formed around it. Because the blank sheet is in touch with two areas, this process is called two point incremental forming. There is a partial die used in TPIF in the figure 2.5 which provides more flexibility because with a little change in the die different but similar parts can be produced. Sometimes a full die is used and it provides better support for critical areas under the blank but the flexibility will be lower because only one type of product can be processed in this type of TPIF [14, 15].

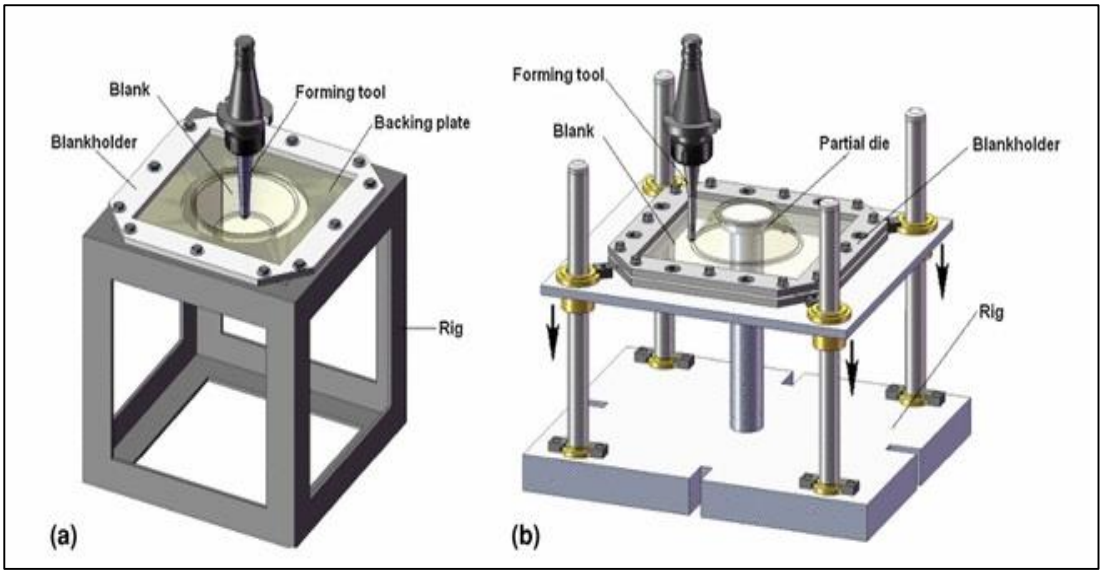

Figure 2.5: Illustration of TPIF: (a) Downward, (b) Backward [15].

Another type of TPIF is developed recently. DSIF or double sided incremental forming in which one tool is used on either side of the sheet. One tool acts as the forming tool and the other acts as a local die or support at each deformation point. It is shown that the geometric accuracy achievable in DSIF is significantly better than with any other form of incremental forming. Furthermore, the characteristic of the absence of any shape specific tooling is preserved. Additionally, the geometric complexity of components formable is significantly greater and the formability is also greater with DSIF. One big problem with ISF is geometrical accuracy which is illustrated in the figure 2.6.

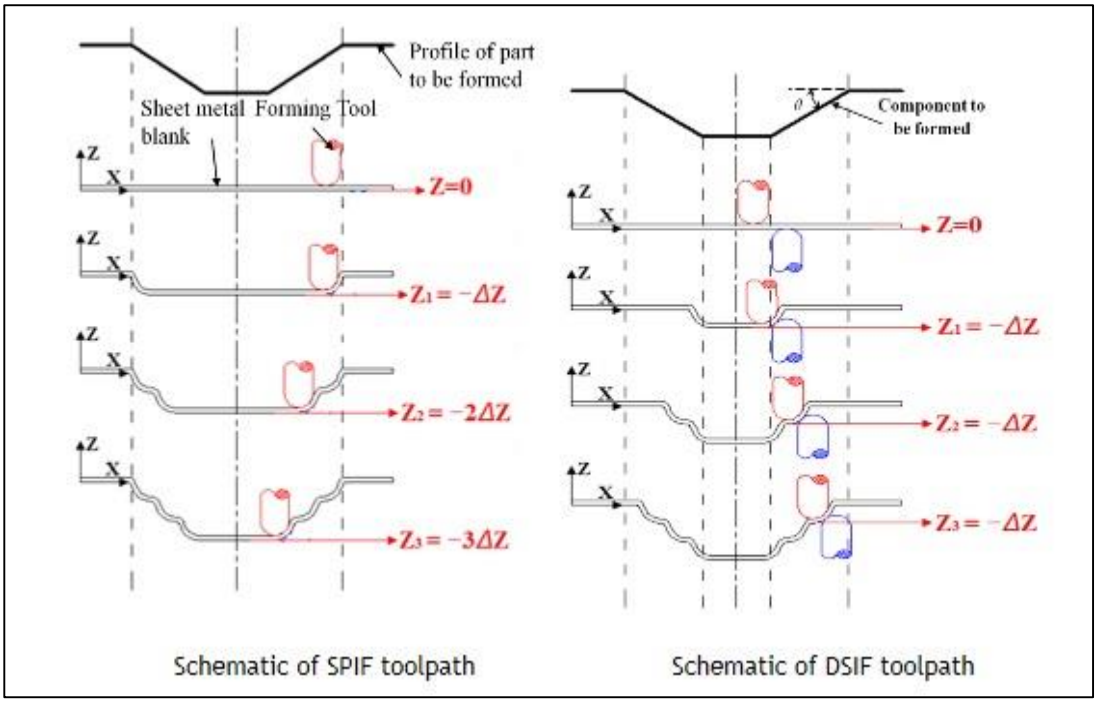

Figure 2.6: Schematics of SPIF and DSIF [16].

When tool moves to deform the sheet an error of Δz occurs along moving to the next step down plain. Because of the essence of ISF this error occurs in every step down and further we go down the error gets bigger. In DSIF the gap between two tools are constant so this error will be constant too. In other words geometrical accuracy in DSIF is better than conventional ISF. DSIF is only available with robotic production or some semi-robotic equipment due to its need for manipulating both tools simultaneously [16].

## 2.3 SPIF Formability

As said before higher formability is one of the advantage points of incremental forming in comparison with other conventional sheet metal forming processes. Some researches proves that conventional forming limit diagrams are not reliable in failure prediction of SPIF due to increased formability of the process. In order to measure the formability of SPIF and reach a better failure prediction for SPIF Iseki represented a

method called incremental sheet metal bulging [17]. Some explanations for increased formability are listed below:

### 2.3.1 Strain Path

Before using the MK model researchers believed that higher formability is the result of non-monotonic serrated strain paths. An example of this kind of behavior is represented in the figure 2.7 [18].

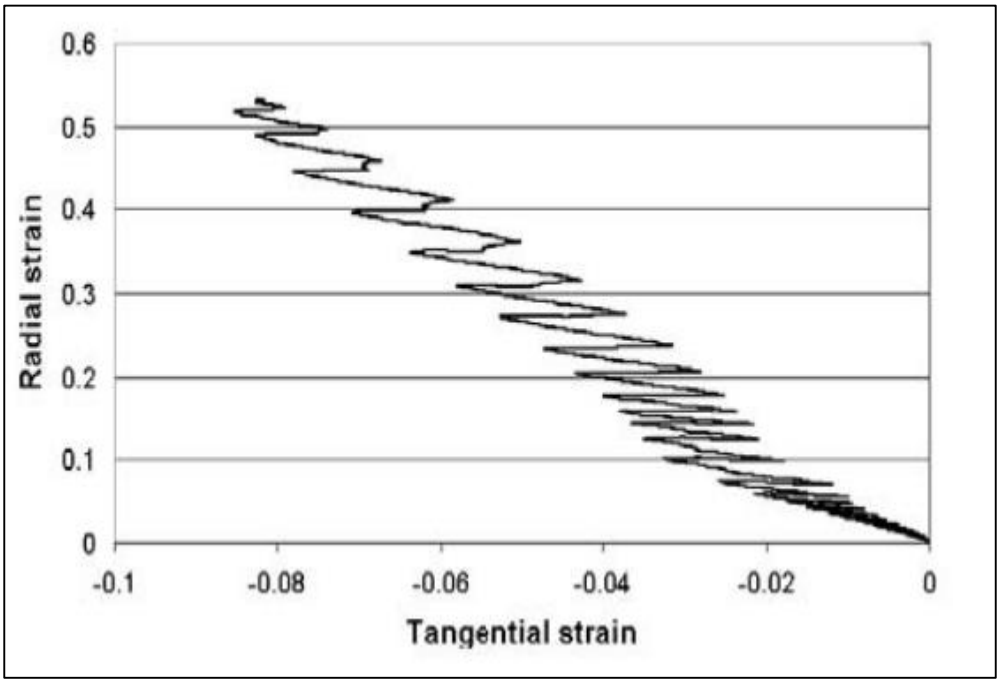


Figure 2.7: Serrated strain path achieved by Mk model [20].

The main reason why this graph was represented is when the tool with small diameter get closer to the selected element passes over it and gets away continuously increasing the level of the deformation in the meantime. The graph shows the radial strain which is very close to principal strain in function of minimum strain or tangential strain of an element on the top side of a SPIF made cone part. This diagram shows how different is the formability of SPIF with other metal processing methods and corresponding

conventional FLDs. So most of the failure prediction attempts on SPIF formability are based on FEA like a successful research by van bael et al [19].

### 2.3.2 Through Thickness Shear

This phenomenon is one of the main explanations of necking delay in SPIF. In the figure 2.8 the coordination system is centered in the tool representing directions n, t and g.

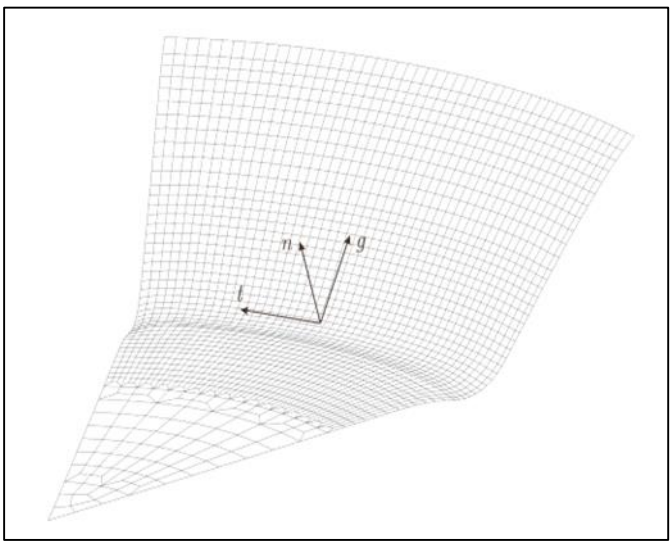


Figure 2.8: N, t and g directions corresponding to Emmens study. [21]

Emmens [21] represented a shearing mechanism that occurs in the plane having directions n and g. briefly the research is based on strain calculation on implementing the shear mechanisms and clearing that despite the fact that necking is the major reason of the failure in a simple tensile test but in a material under a shear load necking may not occur or it may happen the locations other than necking caused by some microscopic behaviors.

### 2.3.3 Bending

The research by Emmens proves that bending in companion with stress can lead to higher stretching causing higher formability [22, 23].

### 2.3.4 Triaxiality

Triaxiality is a ratio playing a specific role in formability behavior of different processes. A recent research by Martin's shows that this ratio in SPIF is significantly lower than other conventional sheet forming processes and a reason of higher formability. And also it shows that this ratio is the highest in the edges among the other element which shows why most of the parts fails in those regions. This research was done by FEA [24].

Each four of above individually cannot prove the higher formability of SPIF in this scale. And there is no comprehensive reason reported yet. But a combination of these reasons and also compression stress can increase the strain level dramatically and explain the formability behavior.

## 2.4 Multi Stage Incremental Forming

The maximum angle of a material can be reached through a simple cone shaped test. In the cone shaped incremental forming the angle of forming changes continuously. Failure occurs when the angle of forming reaches a critical value. This test should be performed when all other parameters of process like feed rate, step size, tool diameter and etc. are constant. The maximum wall angle (see figure 2.9) achieved with this test limits the forming issue due to sine law.

$$t_f = t_o \sin \alpha \quad [25] \qquad \text{Eq.2.1}$$

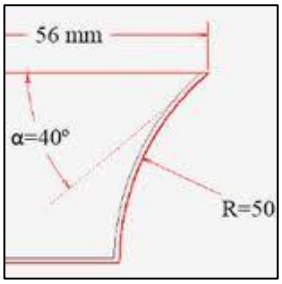

Figure 2.9: Maximum forming angle test [25].

According to the sine law it is impossible to form a vertical wall on the sheet (90 degrees). $t_f$ in the sine law is the thickness achieved in every angle of α and $t_o$be the initial thickness of the sheet. As seen $t_f$ is zero when α equals to zero. To increase the maximum wall angle, the initial thickness of the sheet can be increased but obviously this strategy has limitations on the maximum machine load and overall part thickness specifications. The diameters of the tool and the selected step down also have an influence on the maximum forming angle [25]. Maximum wall angle for different materials are in the table 2.1 [26].

Table 2.1: Maximum forming angle for different materials using SPIF [26].

| Material | Thickness (mm) | Tool Ø (mm) | Max. wall angle (°) |
|---|---|---|---|
| Al3003-O | 1.2 | 10 | 71 |
| Al3003-O | 2.0 | 10 | 76 |
| AA3103 | 0.85 | 10 | 71 |
| AA3103 | 1.5 | 10 | 75 |
| Ti Grade 2 | 0.5 | 10 | 47 |
| DC01 | 1.0 | 10 | 67 |
| AISI 304 | 0.4 | 10 | 63 |

In order to reach higher angles and corresponding formability multi stage incremental forming is applied. In this method instead of reaching the desired angle in one stage the whole process is divided into several stages. With support of a back plate the sheet deforms into a certain angle in each stage and finally get to the desired one that can be

a vertical wall. Of course in this process because the material is continuously flows into the bottom preventing the thinning effect which is the main source of failure in SPIF though provides a more homogeneous thickness distribution throughout the sheet.

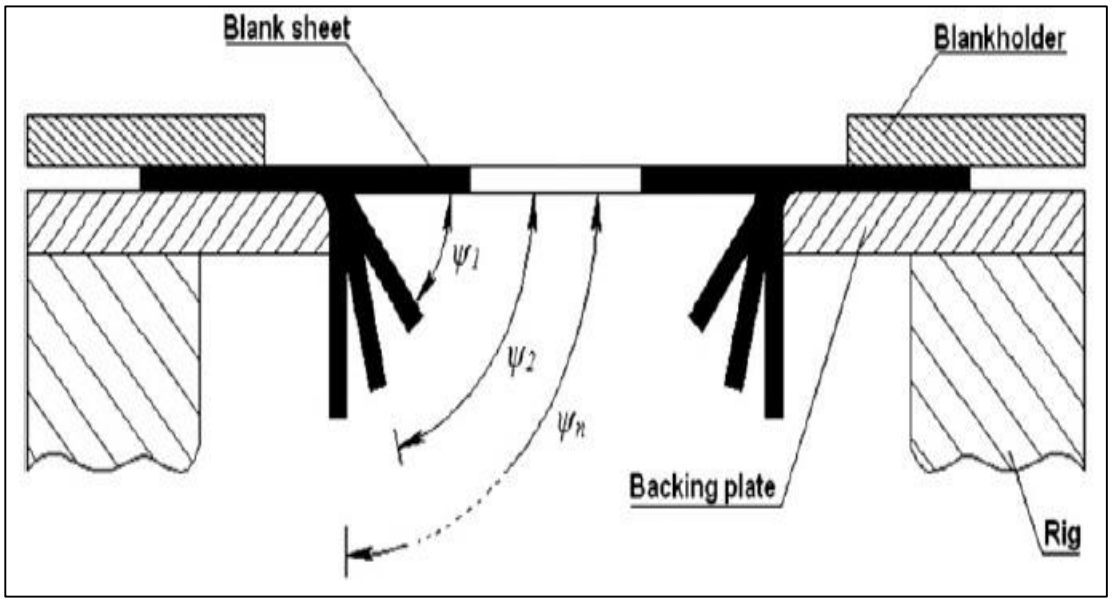

Figure 2.10: An illustration of Multi stage incremental forming [27].

As shown in the picture 2.10 the setup of the process is the same as SPIF. The sheet is fastened in the rig and a back plate supports it. But this time in the first stage, the tool moves on the sheet forming it into angle Ψ1. After finishing the first stage tool moves up to the initial position and starts to form the sheet into angle Ψ2. This process goes on until reaching the desired angle of $\Psi_n$.

Beyond all the things that matters for SPIF and also matters for multi stage incremental forming, the most significant factor involved in multi stage incremental forming is the tool path strategy. Of course what makes it different with conventional SPIF is tool path strategy too. Most of the time this kind of sheet forming process takes on forming

vertical walls which is impossible to get by conventional SPIF. A significant defect called pillow defect occurs when forming the sheet into some angle. Of course many parameters are involved in this defect. Multi stage incremental forming is not an exception too and also it's much obvious in reaching to $90^{o}$ walls. Most of the time a big pillow defect emerges in the bottom of the part during the process.

In order to get rid of this defect a hole is applied in the middle of the material. From that moment the process is called hole flanging which is the process of making a vertical walled part with a hole in the middle of it. It's essential to note that the hole size is not only has effect on pillow defect and also in stress distribution and thickness.

### 2.4.1 On The Formability Of Hole Flanging

Hole flanging is a process in which the material with a hole inside placed in a blanked holder deformed to produce a vertical walled part. The hole can be cut through various methods such as LBM, EDM, wire cut and etc. Hole flanging is vastly used for press working operations and greatly investigated since 1960 by Mackerle [27]. Now days hole flanging is mostly performed by incremental forming due to providing higher formability using multistage strategies. The formability behavior of the SPIF was briefly discussed before, the formability of multistage incremental forming is much more complex due to various stages included in the process [27]. Some of the most significant parameters affecting the formability of the process are as follows:

#### 2.4.1.1 Limiting Forming Ratio

Most of the researches on the hole flanging by press working is done by Mackerle [35]. The results shows that generally the deformation of the sheet with a hole inside is a combination of stretching and bending and also failure occurs by necking or tearing because of excessive strains at the corners. A parameter is introduced here

called LFR which is the maximum part diameter over initial hole diameter. LFR is the limiting forming ratio.

$$LFR = \frac{d_{max}}{d_o} \quad [27] \qquad \text{Eq.2.2}$$

The LFR is greatly dependent on the mechanical properties of the material, surface quality of the inside hole, lubrication and etc. LFR is introduced as a formability factor for hole flanging. Recent research by Silva [37] shows that favorable LFR is obtained when the FFL (fracture forming limit line) diagram of the material is well placed above the FLC (forming limit curve) diagram leading to increased formability (see figure 2.11).

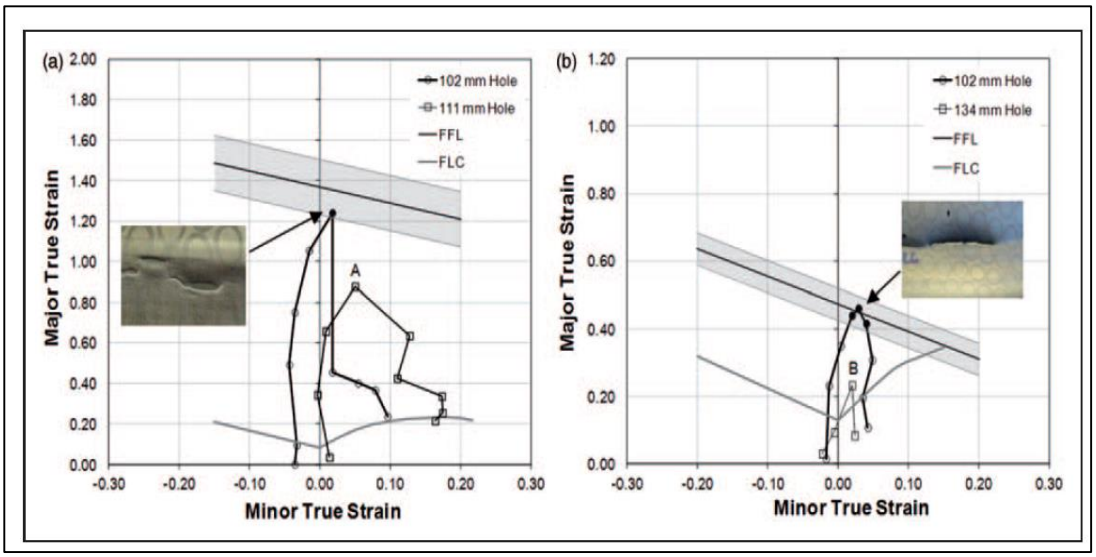


Figure 2.11: LFR and its relationship with FFL and FLC diagram [37].

### 2.4.1.2 Multi stage Incremental Forming Strategies

Recent research by Cui and Gao [28] has represented 3 main strategies for multi stage incremental forming with hole or hole flanging (see figure 2.12). All of them are composed of different stages which is the soul of multi stage incremental forming.

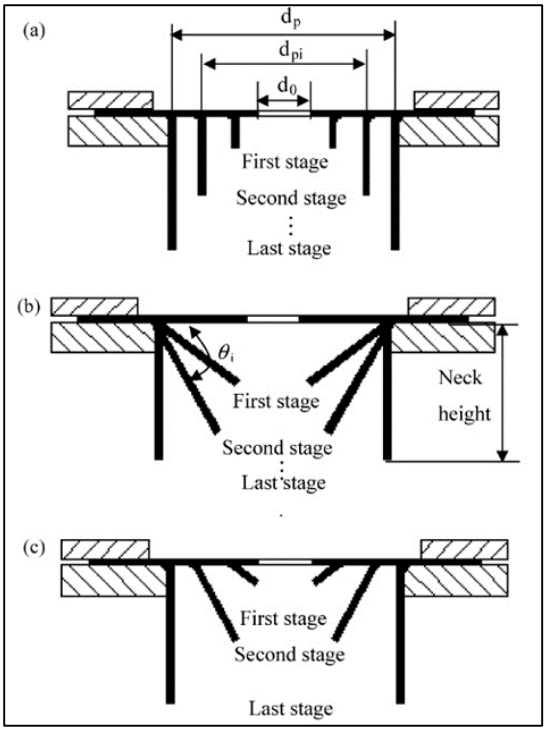

Figure 2.12: Different strategies for multistage incremental forming [28].

In all strategies $d_o$ is the hole size. In strategy 'a' the first stage is diameter of $d_{p1}$ and also angle of 90 degree. After finishing this stage the second one's diameter is $d_{p2}$ and angle 90. In all stages the angle is constant and vertical and the only difference is the diameter of the contours in each stage. Of course using this strategy demands different back plates and constantly changing them after completing each stage according to the stage contour diameter.

In strategy 'b' the diameter of all stages are constant and equals to final diameter of the part. The angle of forming changes in each stage until reaching the vertical wall or 90 degrees.

In strategy 'c' not only the diameter of the contours increases as finishing each stage but also the angle of forming increases too. Until reaching the 90 degrees. This strategy is a combination of previous ones.

The results shows that the maximum depth achieved in strategy ‘c’ is the highest leading to greater formability. Strategy ‘a’ is second and the third is b. the reason why strategy c leads to higher formability is the forming phenomenon. In strategy c not only the incremental forming is involved but also bending is involved too. In each pass a significant amount of bending is applied on the sheet which leads to greater formability instead of rising the stress level in the whole part [28].

#### 2.4.1.3 Number Of Stages

Number of stages is one of the key factors in designing a multi stage SPIF. Because of the soul of the process, deformation mechanism is composed of different stages. Consider a 2 stage method in which the sheet is deformed to 45 degree first and then carries on to the final 90 degree. A big jump between first stage and the second one can cause sheet rupture due to excessive deformation and high stretching the material. In this case the material fails before finishing the whole process. This failure can expressed by thinning effect. When the number of stages are low for example 2 stages of 45 and 90 degree, when the material goes under load of 90 degree a high volume of material starts to flow inside the sheet providing a portion of sheet higher thickness and a portion of it very lower thickness. This lowering thickness goes on until thinning happens in that sector and material fails. On the other hand as the tool moves on the sheet work hardening occurs. The material gets strengthen requiring more stress to get deformed. But if the number of stages is high this could lead to failure because of extreme work hardening on the sheet. The material gets though and if the required amount of stress for deformation is provided instead of deforming, the material fails. In order to benefit from higher number of stages to prevent big jumps between the stages and rupturing the sheet and also benefit the lower number of stages and decrease

the amount of work hardening and failure a reasonable number of stages should be applied. Most researchers recommend 3 or 4 stages for forming a vertical wall [27].

# Chapter 3

# ABAQUS FINITE ELEMENT MODELING

## 3.1 General Description

The finite element is a method where the model is converted to numerical and algebraic equations. The leading equation is an equilibrium one and can be dynamic or static. Two time depending equations can be used for solving the problems: implicit and explicit [29].

### 3.1.1 Implicit Method

In implicit method after dividing the time steps an estimation is made for velocities of nodes at the beginning of each time step. And then the final velocities at the end of the time step will be achieved. These velocities are related to dispositioning which can be referred as strains and corresponding stresses will be calculated. Stability is one the advantages of this method meaning that there is always a stable solution for the mentioned equations no matter how long or short the time period is. Disadvantage point of this method is that the software should make some irritations on the time scale so the software should solve bigger equations. Each time step will demand high computational capacity and will be time consuming [30].

### 3.1.2 Explicit Method

Calculating initial nodal velocities then getting the final velocities and reaching to strain and stress values are just like implicit method. The only difference is in the implicit method every equation should be transformed into an equilibrium one. But in the explicit method some equations never satisfy it. This work is done in order to keep the picked amplitude lower than a critical value. This will eliminate high number of irritation we had before in implicit method and provide us with lower computational requirement for calculating the step time [30].

## 3.2 Considerable Parameters In FEA Method

### 3.2.1 Mass Scaling

The computation time is a very important factor in all the simulation problems. If this time is very high for example 1 month this won't make any sense. Very high analysis time has other problems too. It will increase the chance of undesired errors and also CPU blackouts during the analysis. Consider the computer stops working after 25 days of analysis. That can only described by the word 'disaster'. In order to reduce the computation time a technique is introduced called mass scaling.

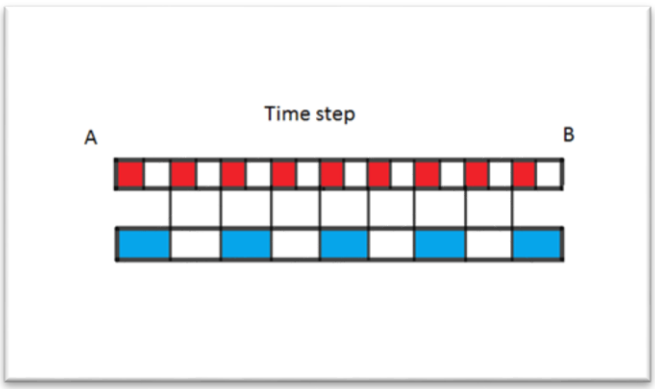


Figure 3.1: Motion of a car from point A to B and its corresponding time increments.

Consider we want to simulate the motion of a car from point A to point B (see figure 3.1). Abaqus calculates each time increment via the formula below:

$$\Delta t = L_{min} \cdot \sqrt{\rho / E} \quad [30] \qquad \text{Eq.3.1}$$

Where Δt is the minimum time increment, L is the minimum element length, ρ is the density of the car and E is young's modulus. With this formula abaqus divides the whole t time of the motion into small increments. Each increment will be calculated and the process will go on until reaching to the destination. This Δt is represented by red line in the figure. Now if the density of the material get scaled by a factor of $f^2$, the minimum time step will be scaled to f. for example if the scaling factor is 4 the time scale factor would be 2. This means the computation time spent to analize each time increment of red line now will be spent for the blue one. So the whole process time will be half of the first try. Ofcourse this computation time wont be exactly half in real case because the process time not only depends on mass scaling factor but also on many other parameters, but it will greatly reduce the analysis time. This technique has no significant effect on precision and widely used for simulations [30,31].

### 3.2.2 Time Scaling

Time scaling is also widely used in simulations. Decreasing the total time of the car motion from A to B in the previous example will greatly decrease the analysis time. Time scaling is only used for non viscous materials where the stresses are independent of strain rate [30].

### 3.2.3 Finite Element Type

One of the key factors to achieve the desired accuracy and also reasonable analysis time is choosing the right element type for the material. Different element types and their corresponding analysis duration are listed in The table 3.1.

Table 3.1: Using different element types for SPIF and their corresponding process times.

| Element type | CPU time (hr) |
|---|---|
| C3D8 | 17.6 |
| C3D8R | 15.4 |
| C3D8R enh. | 28.3 |
| C3D8H | 48.1 |
| C3D8I | 34.9 |
| C3D8IH | 103.3 |
| C3D8RH | 50.9 |
| S4R | 7.3 |

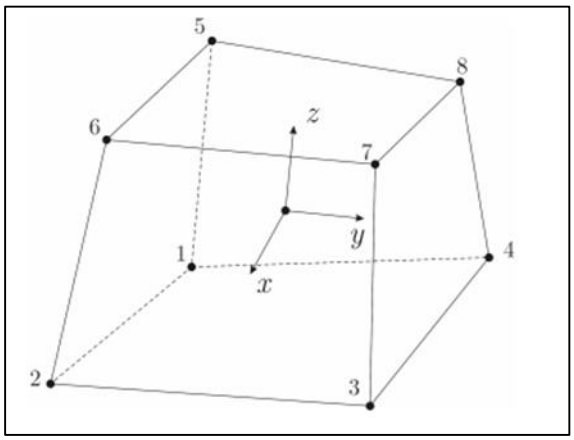


Figure 3.2: An 8 node 3D element used in ABAQUS [30].

As seen in table 3.1 the elements which their names start with C3D8 are 3D 8 node ones (see figure 3.2) and the elements S4R is a shell element which has 4 node (see figure 3.3). The lowest process time is achieved in using shell element because of the

elimination of the third components of stresses and strains so lower computation requirements. Element on the 3rd dimension are necessary if the high percision is required for calculating the exact amount of stresses and strains. But some researchers reccommends using shell element for incremental sheet forming simulations due to providing good percision and lower analysis time.[32,33].

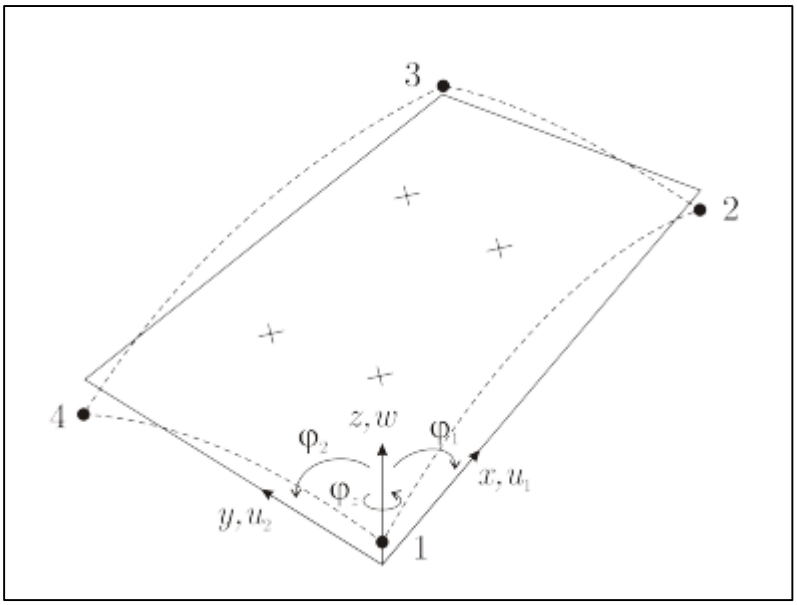


Figure 3.3: A 4 node shell element used in ABAQUS [30].

### 3.2.4 Yield Criteria And Laws

*Von mises yield criterion:*

This criterion is the widest used in simulations du to simplisity. The material is considered isotropic and the overall stresses are calculated via formula below:

$$\sigma_{eq}^2(\underline{\underline{\sigma}}) = \frac{1}{2}\Big[(\sigma_{xx}-\sigma_{yy})^2+(\sigma_{xx}-\sigma_{zz})^2+(\sigma_{yy}-\sigma_{zz})^2+ 6\left(\sigma_{xy}^2+\sigma_{xz}^2+\sigma_{yz}^2\right)\Big].$$

Eq.3.2 [33]

### 3.2.6 Mesh Size Sensitivity Test

There are 2 core issues relating to mesh size:

*Accuracy and Analysis time*

It is obvious that as the mesh size gets smaller the accuracy of the resultsa and analysis time will increase. If the researcher is going to use a some kind of work station, super computer or paralel execution so the time factor will be neglectable but in the matter of normal processors that were used in this study time factor is very important. It seems that it is possible to find a mesh size which will provide us with enough accuracy and also a reasonable process time in the matter of hours.

Despite the fact that the element used in the FEA is shell element and 2D, but with using the sum of the strains law it is possible to get the third strain which is thickness. Some researchers have reported that the accuracy of the shell element in SPIF processes is good [32, 33]. So a single stage 45° cone with depth of 25 mm were produced by experiment to get its thickness distribution. On the other hand a set of tests are aranged with different element sizes in ABAQUS in order to get its thickness destribution and compare with the one achieved in the experiment. Utilizing this method an appropriate solution to mesh size influence in the simulation and also the suitable mesh size can be achieved. All the desired elements to study their third strain component are selected in 5 mm rows in order to simplify the element selection due to different element sizes.

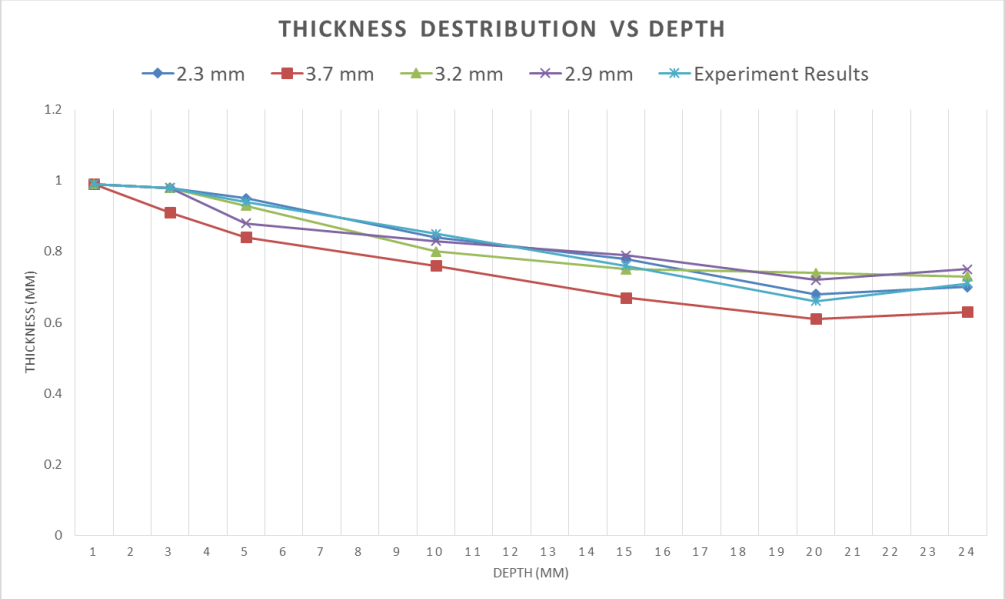


Figure 3.4: Thickness destribution comparison among different element sizes and the actual experiment. Cone 45 degree with hole diameter 80mm. A trend line is used instead of actual scatter points to simplify the comparison.

The difference between big mesh sizes, small ones and the actual thickness profile is obvious in figure 3.4. It can be seen that as predicted the smaller mesh sizes give better results than the bigger ones. If the accuracy of thickness destribution is the center of comparison, mesh size 2.3 gives the best result. Now another set of tests through FEA are carried out to make the circle of mesh sizes smaller and find the best result within the range of 2.3 mm. The aim of this test is to see whether the 2.5 mm mesh size maintain the same desired accuracy or not. The major reason that 2.5 mm mesh size is important is due to the fact that the hole sizes will vary on 5 mm range and using a mesh size which 5 can be divided into that specific amount is important. Consider using a 2.3 mm element size and mesh the sheet, then enlarge the hole in the middle by 5 mm and mesh again. Some elements in the part will have the size of 0.2 mm which will obviously influence in the final results. To get the smooth result this mesh size is critical.

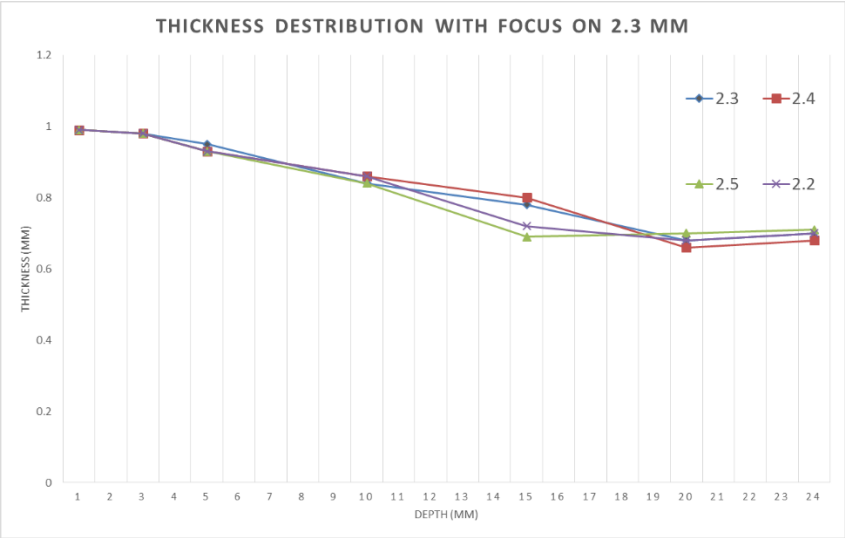


Figure 3.5: Thickness destribution comparison between different element sizes and the 2.3 mm. Cone 45 degree with hole diameter 80mm.

From the Figure 3.5, it is obvious that chnaging the mesh size around 2.3 mm has not a significant effect on the thickness destribution of the parts. So in order to simplify the comparison between selected candidate elements in FEA mesh size 2.5 mm is selected unless some half meshes would remain and selecting the meshes would be extremly difficult. No further reduce in mesh sizes was required because the accuracy provided by 2.5 mm was enough.

# Chapter 4

# METHODLOGY

## 4.1 Experiments

### 4.1.1 Material Properties

The material used for the experiments is an aluminuim alloy sheet which is rolled. It means it is prestrained. The thickness of the aluminuim sheets is 1 mm. Samples were taken in order to perform tensile test and achieving the mechanical properties. These samples are cut through the sheet via a drilling tool and then set into the tensile test machine. A hardness test is done on the samples to determine its hardness too.

Table 4.1: Material properties for Aluminum.

| Material type | Structure | Density | Hardness(BHN) |
|---|---|---|---|
| Aluminuim | M-C | 2.78g/cc | 120 |

The samples for tensile test are cut via drilling tool in a CNC machine and the standard of ASTM A370 is utilized. The samples were cut into 0 and 90 degrees along the sheet.The tests are done in tensile test machine INSTRON. The description of the ASTM 370 standard, the corresponding sample details and a figure of the machine used for obtaining the data are respectively shown in table 4.2, and figure 4.1.

Table 4.2: Description of ASTM 370 standard.

| ASTM 370 Standard | | | |
|---|---|---|---|
| G-Guage length | 50±0.1 mm | A-Length of reduced section | 60 mm |
| W-Width | 12.5±0.25 mm | B- Grip section length | 50 mm |
| R-Radious of fillet | 13 mm | C-Grip section width | 20 mm |
| L-overall Length | 200 mm | T-Tickness | 2 mm |

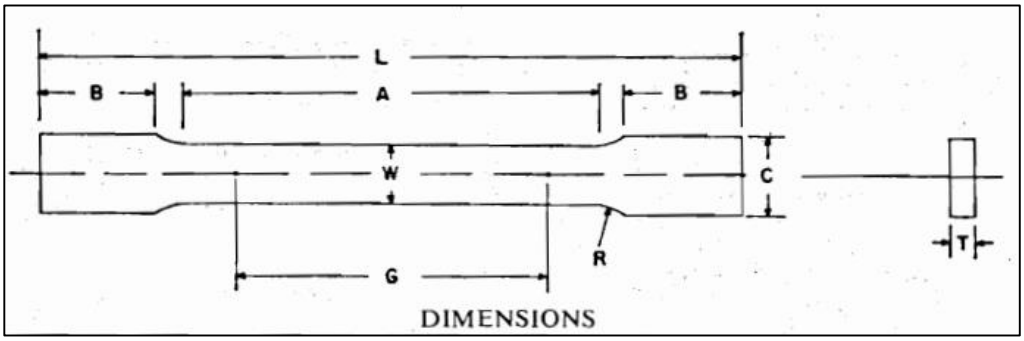


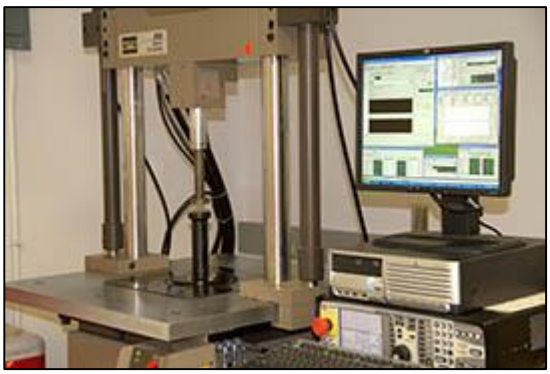

Figure 4.1: Instron machine used for tention test on samples.

After obtaining the stress strain curve of the sheets and calculating the alongation percantage and area reduction of the specimens were calculated with the equation below:

$$A_r = 100 \times \frac{A_o - A_f}{A_o} = 100 \times \left[(W_o \times t_o) - (W_f \times t_f)\right]/(W_o \times t_o) \quad \text{Eq.4.1}$$

$A_r$: Percentage reduction in area

$A_o$: Initial area of cross section of the tention test specimen

$A_f$: Area of cross section at the fracture of sample

$w_o$ & $t_o$ are measured by the original samples and then original cross section area were calculated. $w_f$ & $t_f$ were measured at the neck of fracture using digital vernier clipers with tolearnse of $\pm$0.01 mm. The percantage elongation were calculated using formula below:

$$\%E = 100 \times (l - l_o)/l_o \qquad \text{Eq.4.2}$$

%E is elongation in percantege and l is the final length of the specimens and $l_o$ is the initial length of the specimens. The final properties obtaind for the material is shown in table 4.3.

Table 4.3: Material properties of used Aluminum alloy.

| UTS | 470 MP | Hardness | 120 BHN |
|---|---|---|---|
| $S_y$ | 324 MP | %Elongation | 19% |
| Poisson's Ratio | 0.33 | Elastisity Modulus | 73.1 GPa |

### 4.1.2 CNC Machine

In order to perform the experiments a cnc machine DUGARD EAGLE 760 (see figure 4.2) which benefits from 3 axes is used. This machine has a FANUC controller implemented inside it. The machine description is in table 4.4.

Table 4.4: Properties of the CNC machine used for experiments.

| CNC machine | DUGARD FANUC |
|---|---|
| Number of Axes | 3 |
| Machining Capacity (mm) | 760×430×460 |
| Max tool Diameter (mm) | 89 |
| Max spindle speed (rpm) | 8000 |


Figure 4.2: Dugard Eagle 760 CNC machine.

### 4.1.3 Tooling

The forming tool is made of HSS with hardness of 60-65 HRC. The tool head is spherical and its diameter is 14mm. Utilizing a tool with this material has some benefits such as:

- Superior wear resistance
- High toughness
- Good dimentional stability
- High compressive resistance

The tool is mounted to a normal milling tool holder shank.

### 4.1.4 Fixture System And Rig

The fixture is specially designed and built for incremental forming. It is made of steel for maximum strength. As illustrated in the figure the fixture is supported by 4 steel rods which are well placed to reduce the vibrations as much as possible and provide the system to stand firmly. Also it will help to resist to unwanted forces and tentions. There is a back plate placed above the rods. This back plate has the role to support the sheet on it which will be placed. For different purposes of the incremental forming this back plate can be changed for example to implement different forming strategies, tool paths and shapes. As said before the sheet will be placed on the back plate and in order to make the sheet stand firmly during the forming process a plate is mounted on the back plate holding the sheet as tight as possible preventing it from unwanted moving. Every time a new sheet is about to be inserted this support plate should be removed an then placed again. An illustration of fixture and its cross section are illustrated in figures 4.3 and 4.4.

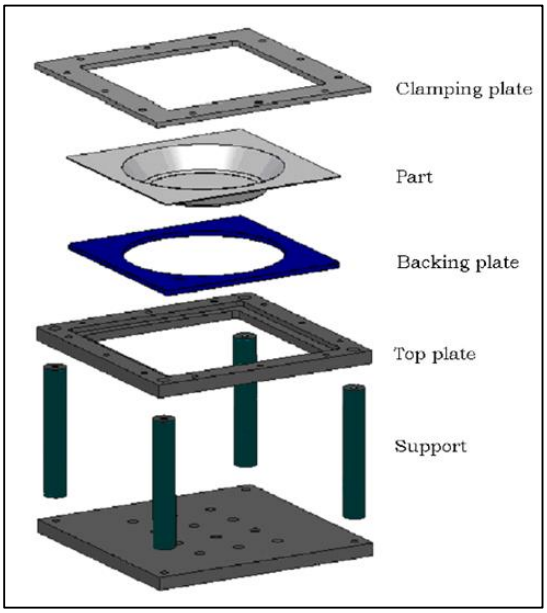


Figure 4.3: An illustration of Fixture system used for incremental forming [24].

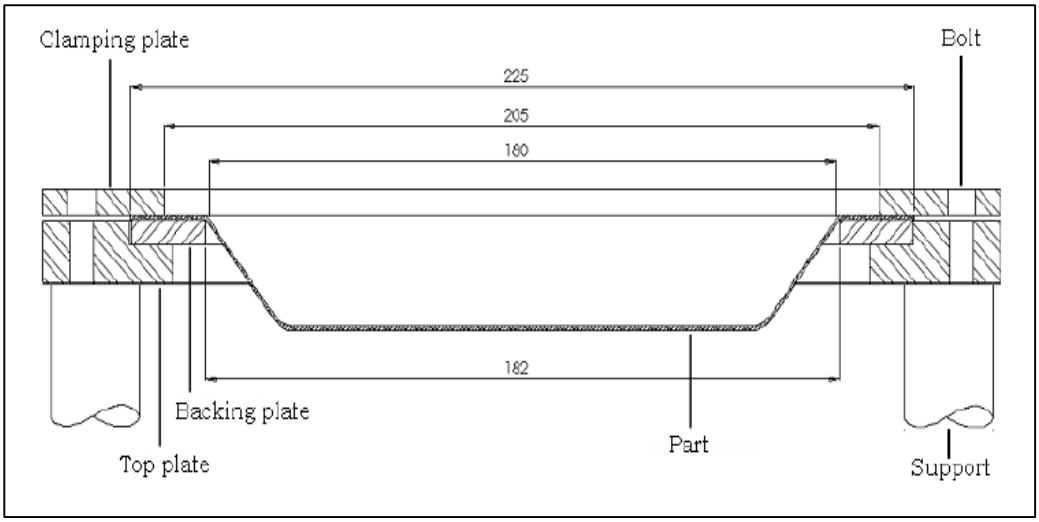

Figure 4.4: The cross section of the fixture used for the experiments.

### 4.1.5 Measurments

The only data that are gonna be extracted from the experiments are thickness distribution, maximum depth and failure locations. For this purpose a normal micrometer and depth guage is utilized. The tolerance of the macrometer is 0.002 milimeter.

### 4.1.6 CAD – CAM

In order to make the parts in the CNC machine a specific tool path should be generated to use as an input to the controller. There are different software packages available to generate this kind of tool path like solidworks, catia, CIMCO and etc. This tool path is generated by POWERMILL software. The tool path is consist of 4 stages which are fixed for 45°, 60°, 75° and 90°. The machine will execute these stages one by one. All stages are in step down form and they will maintain the depth of 40 mm until the failure occures. An illustration of tool path is shown on the figure 4.5. This tool path is illustrated in SIEMENS NX software showing tool path for 45° stage.

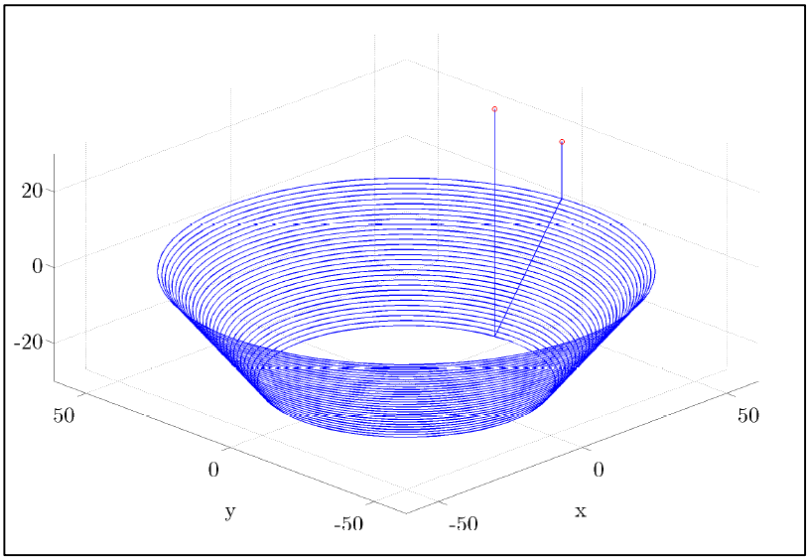

Figure 4.5: An example of tool path generated by POWERMILL to use in CNC machine.

### 4.1.7 Chosen Parameters For Experiments

As mentioned before the purpose of this research is to investigate the effect of hole size in hole flanging made by multistage incremental forming. The selected material is aluminuim alloy. The sheets are cut into 170 mm length and width squares and placed on the made fixture. As mentioned before in the number of stages section less stages will lead to excessive deformation and early failure when aiming to make vertical walls considering the fact that the sheet is already prestrained and unanealed. Also too many stages will make the sheet much more work hardened and in order to perform the deformation more stress is needed, instead of deforming the material it will lead to failure. 4 and 3 stages were investigated before making the final decision and the best results were achieved in 4 stage strategy. So the tool path were set to 4 stages of 45°, 60°, 75° and 90°. The forming strategy were discussed earlier. According to research by Gao the stategy b were chosen because in case of other strategies the results by these one were impossible to be compaired and the whole work would be absurd. In case of step size a normal average stepsize of 1 mm were

chosen because there is no solid proof that the higher or lower stepsize will increase or decrease formability. It is still a debate article among researchers. The feed rate of the tool were set to 70 mm/sec providing an average forming speed. Because in some tries that were done before the actual experiments material removal were observed during them, using of lubrication were seem to be necessary. Tense heat generation and material removal could affect the results considering the 1 mm thickness of the sheet. So a kind of engine oil were used for lubrication and it improved the forming situation significantly.

### 4.1.8 Experimantal Plan

The aim of the article is to study the effect of hole size on different aspects of the hole flanging. For this reason a set of tests were designed to do so. As explained in the previous section, with using mentioned selected parameters, the set of tests are in the table 4.5.

Table 4.5: Table of experiments and their varying hole sizes.

| TEST | Hole Size (Diameter) |
|---|---|
| TEST 1. | 75 mm |
| TEST 2. | 80 mm |
| TEST 3. | 85 mm |
| TEST 4. | 90 mm |
| TEST 5. | 95 mm |

In order to get pure effect of the hole size, all other parameters were kept constant as much as possible. The data extracted from the tests will be thickness distribution and

maximum depth without failure. Aditional data will be added to these via the FEA simulations.

## 4.2 Dynamic Explicit Simulation Via ABAQUS

An FEA simulation were done to gather additional data and also compare with experiment results. In order to set up the simulation some parameters were chosen. Some of these parameters are discussed here:

### 4.2.1 Explicit/ Implicit

The difference between 2 methods were discussed earlier. Because of the nature of the process which is incremental, if the software is able to pick smaller increments it will greatly affect the accuracy of the results. One of the main difference of the 2 methods are picking and organization of these increments which in the implicit method it will be very time consuming. The explicit method was chosen to simulate the processes, not only to save time in calculating incrimination time that has a big deal, but also to improve the accuracy of the whole process.

### 4.2.2 Element Type

Some of the element types and corresponding run time were shown in the table 3.1. Using an 8 node element or 3D element will increase the accuracy of the simulation due to involving the third element of strains and stresses. But also it will greatly increase the total run time of the process.

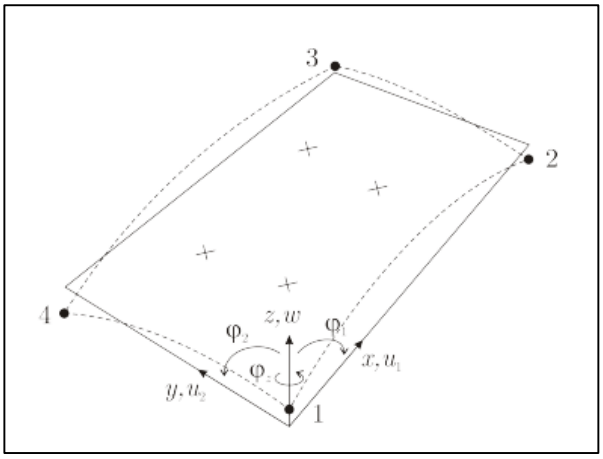

Figure 4.6: The shell element used for FEA simulations.

The research done by Bael [32] and Mackerle [35] shows that using shell elements will provide good accuracy despite the fact that using these element types will eliminate 3rd components of stresses and strains. It is important to note that with 2 strain components in hand it is possible to calculate the third one.

### 4.2.3 Meshing Type

As an element mesh type a shell element in shape of Quad-dominated were chosen. The Triangular elements will reduce the accuracy slightly [32]. This mesh shape is a 4-node doubly curved thin or thick shell, reduced integration, hourglass control with finite membrane strains.

Because of the complexity of the process a very simple meshing were needed which the automatic meshing tool of the software were not capable of doing so. In order to solve this problem some guide lines were used to simplify auto meshing mechanism and avoid complex shapes generation. An illustration of two methods are in the figures 4.7 and 4.8.

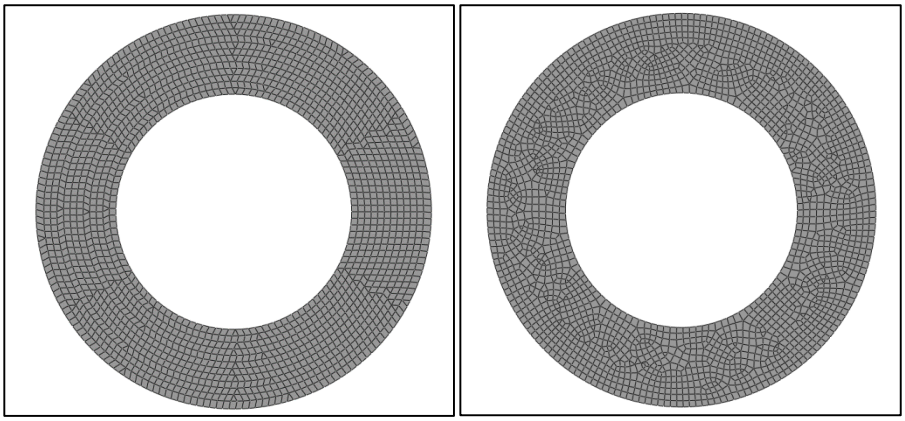

Figure 4.7: Difference between meshing with customized guidelines (Left) and automatic meshing (right).

As seen here with a simple trick the complexity level of the meshing were reduced greatly. It is necessary to mention that in the corrected meshing type, the Quad elements are accompanied by some Tri elements too which were inevitable. As the complexity of the model reduces the chance of having unexpected errors and CPU break downs reduces too. This meshing style will make the mesh selection procedure easier and also the comparison of the results will be more reliable.

Because the tool will face no deformation on it during the process, an element of solid shell were chosen to make it and the meshing type is simple and automatic.

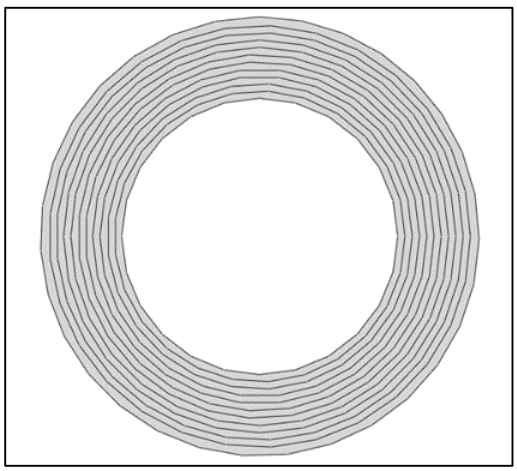

Figure 4.8: The guide lines used for decreasing the complexity of the meshing.

## 4.3 Modeling And Boundary Conditions

The key in the simulation problems is to simplify the process in a way that this simplification won't affect the results significantly [37]. Reducing the parts and parameters in the model will reduce the number of the elements that should be calculated in each increment and will reduce the process time significantly. The model that were used to simulate the hole flanging is illustrated in figure 4.9.

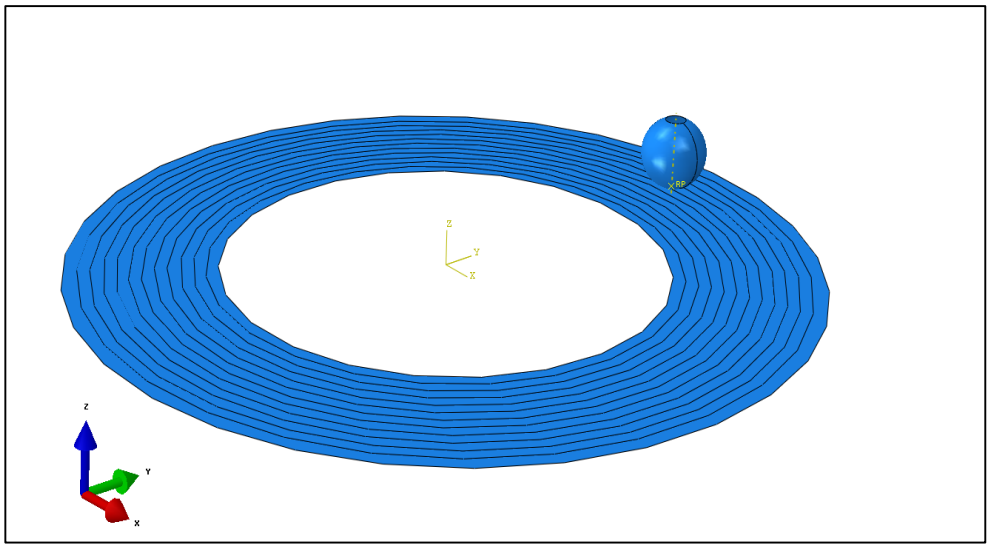

Figure 4.9: The simplified model of Incremental forming in ABAQUS.

It is composed of the sheet with mentioned meshing guide lines which are visible here and also the tool. The tool is simplified to a normal sphere and placed above the sheet. The whole rig or fixture is eliminated from the model and replaced with boundary conditions in order to reduce the element numbers. Instead of the interaction of the back plate and clamping plate the sheet is fully constrained on the edges or so called ENCASRE.

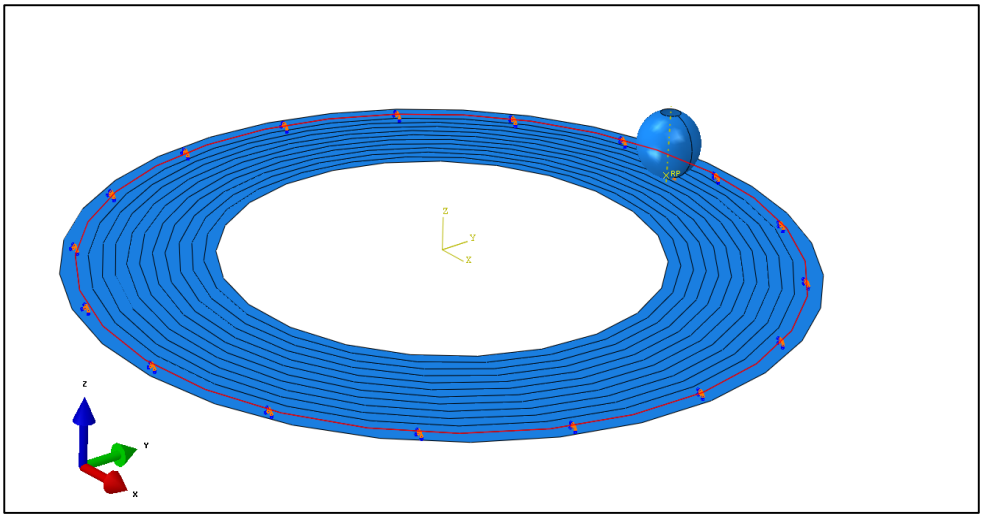

Figure 4.10: The boundary condition of ENCASRE around the sheet representing the simplified fixture.

The freedom degree is reduced to zero on the edges of the sheet while the tool can move towards the 3 axes but cannot rotate (DOF=3).

### 4.3.1 Line Test

Before simulating the real process some simple tests were done to examine the model and corresponding boundary conditions. The most primitive one is line test. Line test is like incremental forming in a very basic level (see figure 4.11).

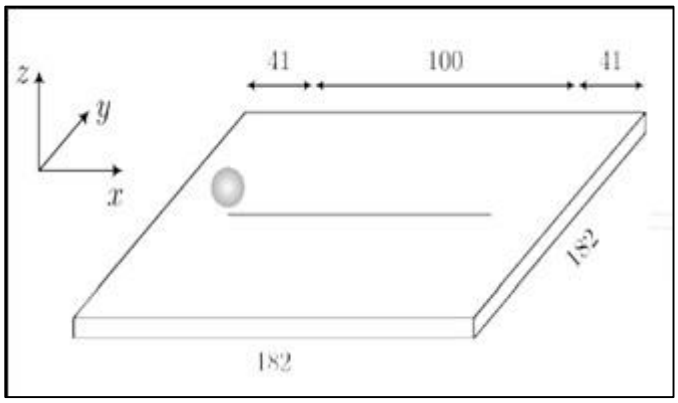


Figure 4.11: An illustration of simple line test to begin with ABAQUS. All the distances are in mm.

The spherical tool will move 100 mm towards the sheet with 1 mm thickness. The element used here is a 4 node shell element.

### 4.3.2 Tool path/ Amplitude

Amplitude in ABAQUS is greatly relied on boundary condition section. In order to move an object, define its velocity or control the movement amplitude is used [30]. In other words in case of incremental forming the tool path is represented by amplitude in ABAQUS. Unfortunately the real tool path used for experiments which were generated via POWERMILL software is not able to be imported to the software. So the whole tool path for the software should be generated manually again. A very fundamental and simple concept as a tweak were used to do so. For example we are trying to generate tool path for 90°cone stage. This tool path is consist of the same circles in different Z levels that are shown in figure 4.12.

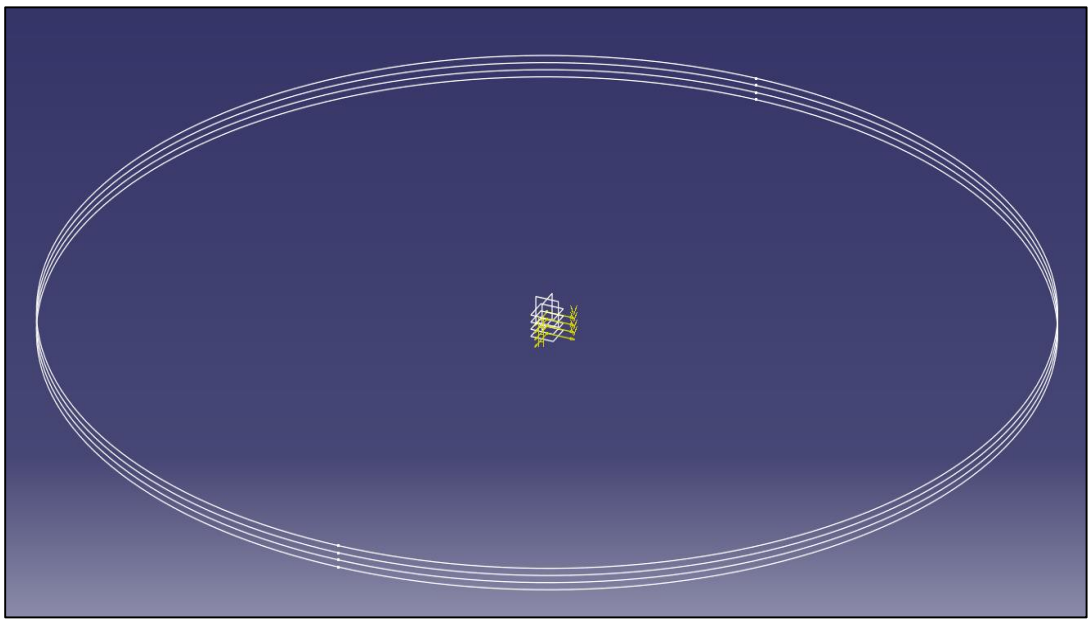

Figure 4.12: Different z levels of contours in 90 degree stage.

Here 4 contours of 4$^{th}$ stage is shown. As seen the whole circles are the same, only different in Z levels. In order to extract the amplitude or tool path the circle should

be divided into several points, with organizing the point's coordination the desired tool path will be generated. A simple way is, with the equation of the circle in hand with hierarchical increase in for example Y the corresponding X will be extracted. This will divide the whole circle into portions as figure 4.13.

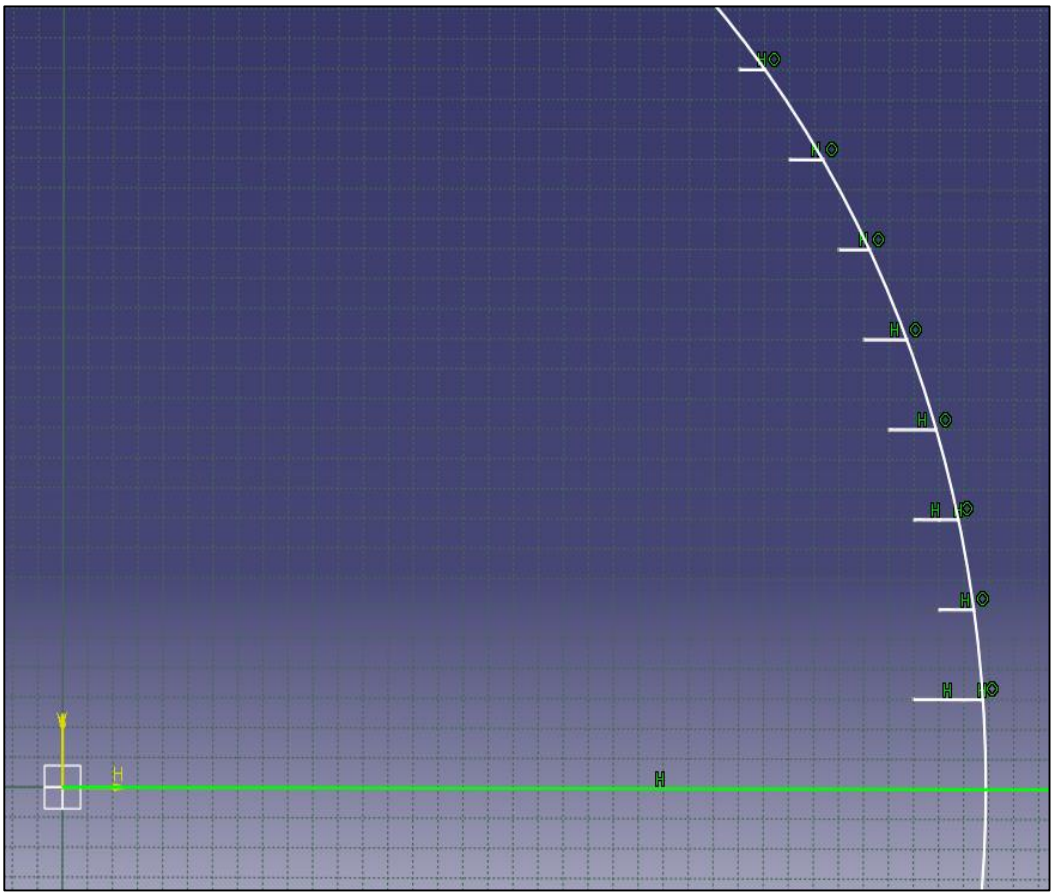

Figure 4.13: Dividing a circle into portions using irritations of Y.

It is obvious that the length of the extracted portions are not equal. This means that if the coordinates achieved by this method is used, with constant time period for each portion the velocity of the tool will be changing constantly. This is not acceptable. So another method is used to generate the coordinates and tool path. In this method instead of constantly changing one parameter of X or Y in the circle equation, we will try to divide the whole circle into equal portions using equal amounts of Θ. With given

constant amount of time period for each portion Θ˙will remain constant and that will provide us with constant linear velocity of the tool (see figure 4.14).

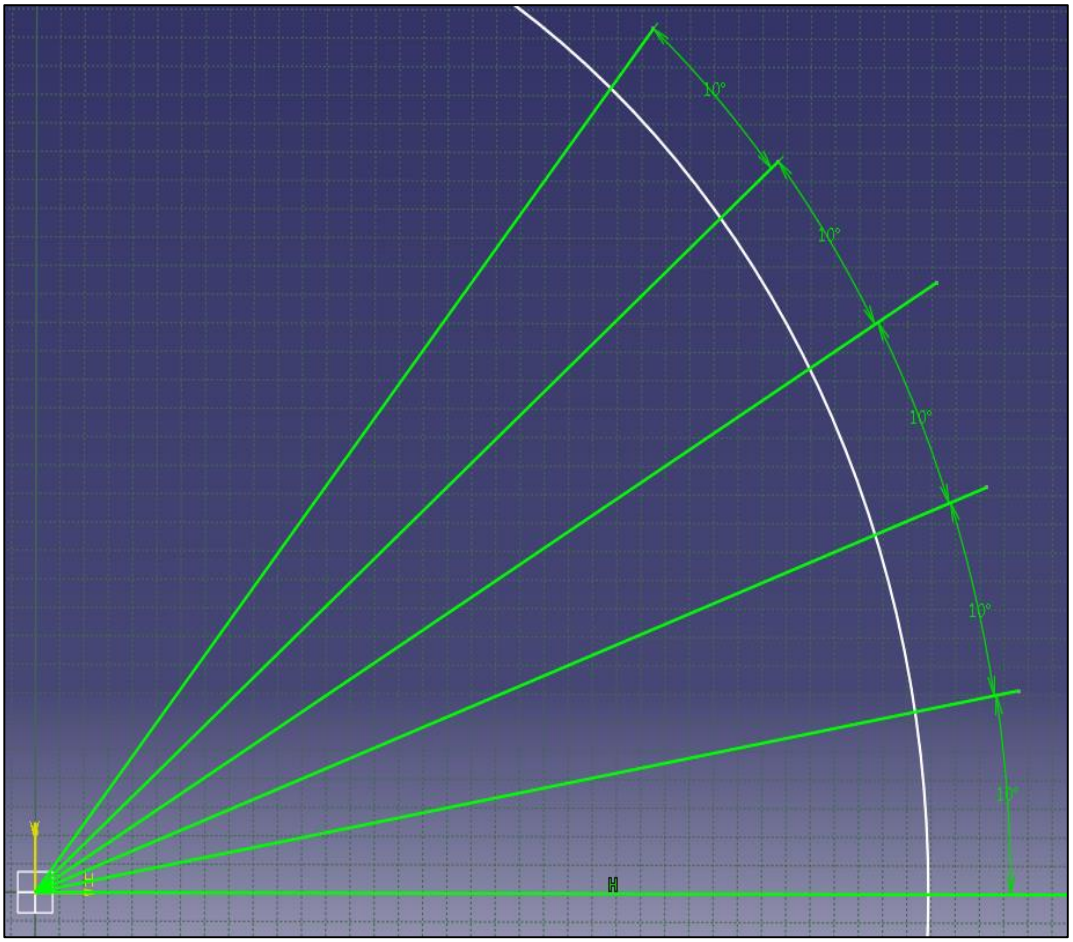


Figure 4.14: Dividing a circle into portions using Irritations of Θ.

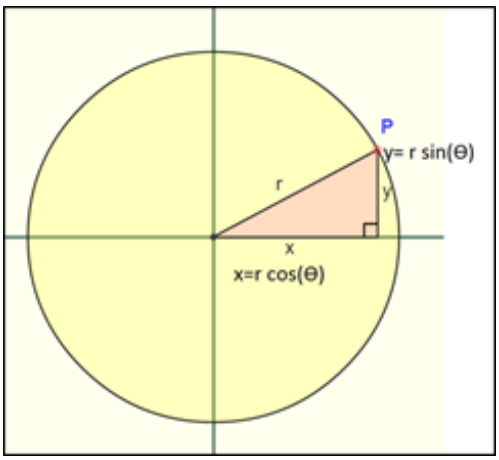


Figure 4.15: The method used for calculating X and Y corresponding to Θ.

Now in order to divide the circle into equal portions using Θ method a simple rule is utilized. With this simple rule and changing the Θ constantly all the coordinates on the circle can be achieved. Finding coordinates for one circle means finishing the whole tool path for 90 degree stage because all contours are the same except their Z level which can be edited when in putting data into ABAQUS.

The same method will be used for other stages tool path. An algorithm is written in excel in order to achieve this goal. Θ step size for all the stages is fixed on 0.1 degree so every contour is consist of 3600 points. Moving the tool among these points continually will make a circle shape like path. That is exactly what the CNC machine compiler does when attempts for a circular interpolation but in higher accuracy of course. An example of the algorithm results is shown in table 4.6.

Table 4.6: The algorithm used in excel to generate amplitude for ABAQUS.

| | A | B | C | D | E | F | G | H | I | J | K | L | M | N | O | P | Q | R | S | T | U | V |
|---|---|---|---|---|---|---|---|---|---|---|---|---|---|---|---|---|---|---|---|---|---|---|
| 1 | 1 | 0.017452 | 1.099502 | 0.999848 | 62.9904 | | | 0.0001 | 1.099502 | | | 0.0001 | 62.9904 | | 0.6301 | 53.5 | | 0.6301 | -34 | | 0.6301 | 0 |
| 2 | 3 | 0.052336 | 3.297165 | 0.99863 | 62.91366 | | | 0.0002 | 3.297165 | | | 0.0002 | 62.91366 | | 0.6302 | 53 | | 0.6302 | -33.68 | | 0.6302 | 0 |
| 3 | 5 | 0.087156 | 5.490812 | 0.996195 | 62.76027 | | | 0.0003 | 5.490812 | | | 0.0003 | 62.76027 | | 0.6303 | 52.5 | | 0.6303 | -33.36 | | 0.6303 | 0 |
| 4 | 7 | 0.121869 | 7.677769 | 0.992546 | 62.53041 | | | 0.0004 | 7.677769 | | | 0.0004 | 62.53041 | | 0.6304 | 52 | | 0.6304 | -33.04 | | 0.6304 | 0 |
| 5 | 9 | 0.156434 | 9.855371 | 0.987688 | 62.22437 | | | 0.0005 | 9.855371 | | | 0.0005 | 62.22437 | | 0.6305 | 51.5 | | 0.6305 | -32.72 | | 0.6305 | 0 |
| 6 | 11 | 0.190809 | 12.02097 | 0.981627 | 61.84251 | | | 0.0006 | 12.02097 | | | 0.0006 | 61.84251 | | 0.6306 | 51 | | 0.6306 | -32.4 | | 0.6306 | 0 |
| 7 | 13 | 0.224951 | 14.17192 | 0.97437 | 61.38531 | | | 0.0007 | 14.17192 | | | 0.0007 | 61.38531 | | 0.6307 | 50.5 | | 0.6307 | -32.08 | | 0.6307 | 0 |
| 8 | 15 | 0.258819 | 16.3056 | 0.965926 | 60.85333 | | | 0.0008 | 16.3056 | | | 0.0008 | 60.85333 | | 0.6308 | 50 | | 0.6308 | -31.76 | | 0.6308 | 0 |
| 9 | 17 | 0.292372 | 18.41942 | 0.956305 | 60.2472 | | | 0.0009 | 18.41942 | | | 0.0009 | 60.2472 | | 0.6309 | 49.5 | | 0.6309 | -31.44 | | 0.6309 | 0 |
| 10 | 19 | 0.325568 | 20.51079 | 0.945519 | 59.56767 | | | 0.001 | 20.51079 | | | 0.001 | 59.56767 | | 0.631 | 49 | | 0.631 | -31.12 | | 0.631 | 0 |
| 11 | 21 | 0.358368 | 22.57718 | 0.93358 | 58.81557 | | | 0.0011 | 22.57718 | | | 0.0011 | 58.81557 | | 0.6311 | 48.5 | | 0.6311 | -30.8 | | 0.6311 | 0 |
| 12 | 23 | 0.390731 | 24.61606 | 0.920505 | 57.99181 | | | 0.0012 | 24.61606 | | | 0.0012 | 57.99181 | | 0.6312 | 48 | | 0.6312 | -30.48 | | 0.6312 | 0 |
| 13 | 25 | 0.422618 | 26.62495 | 0.906308 | 57.09739 | | | 0.0013 | 26.62495 | | | 0.0013 | 57.09739 | | 0.6313 | 47.5 | | 0.6313 | -30.16 | | 0.6313 | 0 |
| 14 | 27 | 0.45399 | 28.6014 | 0.891007 | 56.13341 | | | 0.0014 | 28.6014 | | | 0.0014 | 56.13341 | | 0.6314 | 47 | | 0.6314 | -29.84 | | 0.6314 | 0 |
| 15 | 29 | 0.48481 | 30.54301 | 0.87462 | 55.10104 | | | 0.0015 | 30.54301 | | | 0.0015 | 55.10104 | | 0.6315 | 46.5 | | 0.6315 | -29.52 | | 0.6315 | 0 |
| 16 | 31 | 0.515038 | 32.4474 | 0.857167 | 54.00154 | | | 0.0016 | 32.4474 | | | 0.0016 | 54.00154 | | 0.6316 | 46 | | 0.6316 | -29.2 | | 0.6316 | 0 |
| 17 | 33 | 0.544639 | 34.31226 | 0.838671 | 52.83625 | | | 0.0017 | 34.31226 | | | 0.0017 | 52.83625 | | 0.6317 | 45.5 | | 0.6317 | -28.88 | | 0.6317 | 0 |
| 18 | 35 | 0.573576 | 36.13532 | 0.819152 | 51.60658 | | | 0.0018 | 36.13532 | | | 0.0018 | 51.60658 | | 0.6318 | 45 | | 0.6318 | -28.56 | | 0.6318 | 0 |
| 19 | 37 | 0.601815 | 37.91435 | 0.798636 | 50.31404 | | | 0.0019 | 37.91435 | | | 0.0019 | 50.31404 | | 0.6319 | 44.5 | | 0.6319 | -28.24 | | 0.6319 | 0 |
| 20 | 39 | 0.62932 | 39.64718 | 0.777146 | 48.9602 | | | 0.002 | 39.64718 | | | 0.002 | 48.9602 | | 0.632 | 44 | | 0.632 | -27.92 | | 0.632 | 0 |
| 21 | 41 | 0.656059 | 41.33172 | 0.75471 | 47.5467 | | | 0.0021 | 41.33172 | | | 0.0021 | 47.5467 | | 0.6321 | 43.5 | | 0.6321 | -27.6 | | 0.6321 | 0 |
| 22 | 43 | 0.681998 | 42.9659 | 0.731354 | 46.07528 | | | 0.0022 | 42.9659 | | | 0.0022 | 46.07528 | | 0.6322 | 43 | | 0.6322 | -27.28 | | 0.6322 | 0 |
| 23 | 45 | 0.707107 | 44.54773 | 0.707107 | 44.54773 | | | 0.0023 | 44.54773 | | | 0.0023 | 44.54773 | | 0.6323 | 42.5 | | 0.6323 | -26.96 | | 0.6323 | 0 |
| 24 | 47 | 0.731354 | 46.07528 | 0.681998 | 42.9659 | | | 0.0024 | 46.07528 | | | 0.0024 | 42.9659 | | 0.6324 | 42 | | 0.6324 | -26.64 | | 0.6324 | 0 |
| 25 | 49 | 0.75471 | 47.5467 | 0.656059 | 41.33172 | | | 0.0025 | 47.5467 | | | 0.0025 | 41.33172 | | 0.6325 | 41.5 | | 0.6325 | -26.32 | | 0.6325 | 0 |
| 26 | 51 | 0.777146 | 48.9602 | 0.62932 | 39.64718 | | | 0.0026 | 48.9602 | | | 0.0026 | 39.64718 | | 0.6326 | 41 | | 0.6326 | -26 | | 0.6326 | 0 |
| 27 | 53 | 0.798636 | 50.31404 | 0.601815 | 37.91435 | | | 0.0027 | 50.31404 | | | 0.0027 | 37.91435 | | 0.6327 | 40.5 | | 0.6327 | -25.68 | | 0.6327 | 0 |
| 28 | 55 | 0.819152 | 51.60658 | 0.573576 | 36.13532 | | | 0.0028 | 51.60658 | | | 0.0028 | 36.13532 | | 0.6328 | 40 | | 0.6328 | -25.36 | | 0.6328 | 0 |

### 4.3.3 Cone Test

After performing the line test and also generating the tool path for each stage a simple cone of 45° was made. A cone is a common shaped part to produce via incremental

forming. In order to speed up the process a mass scaling factor of 49 was used. The whole test was deform the sheet into 45° cone successively with 35 contours spacing 1 mm with each other just like the actual simulation (see figure 4.16). In this case a 4 node shell element S4R were used. The time scale is twice as much as the actual analysis in order to speed up the test.

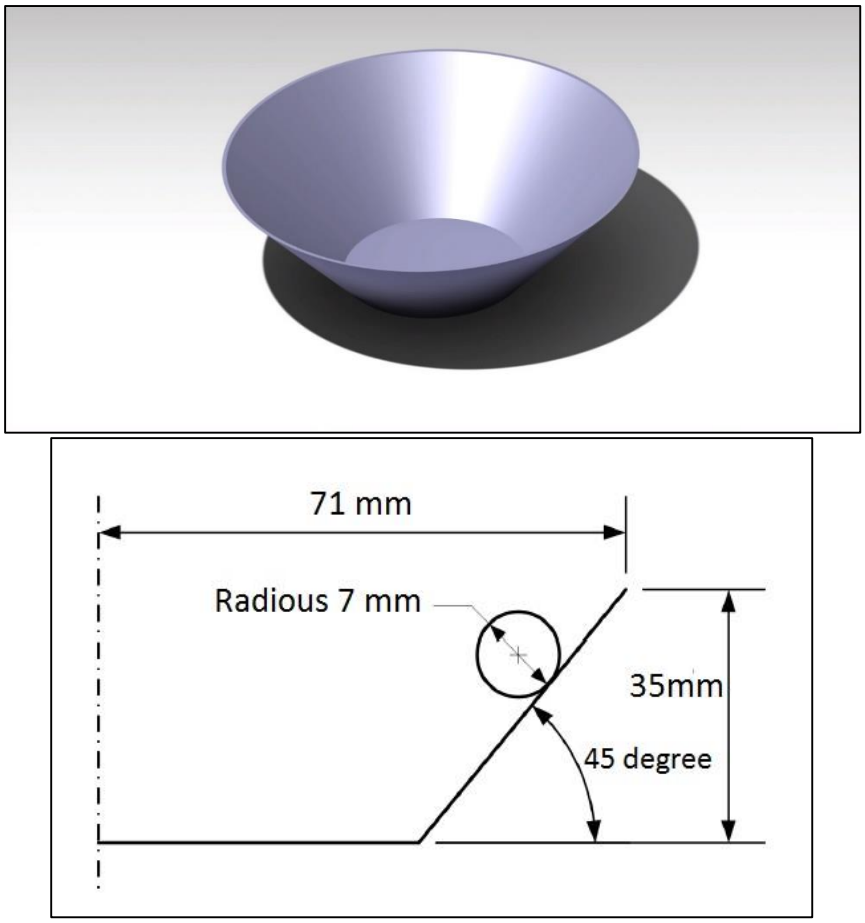


Figure 4.16: 3D view and dimensions of the test for 45° cone. Illustrated using SIEMENS NX.

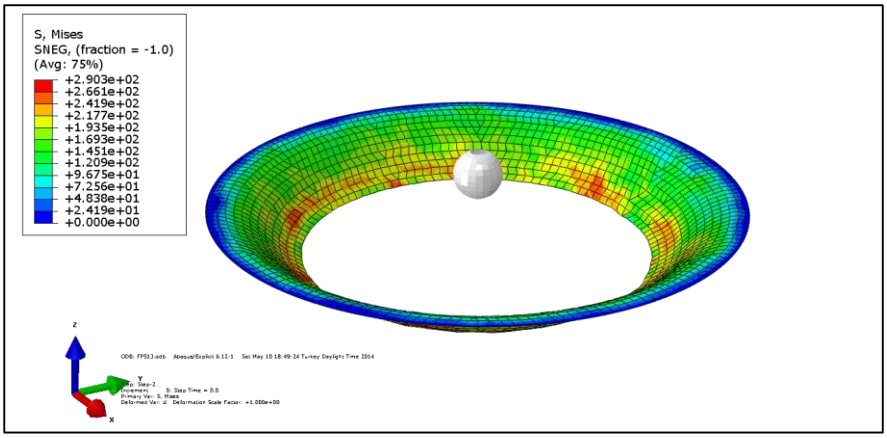

Figure 4.17: The 45° cone simulated by ABAQUS. V.Misses stress (MPa).

### 4.3.4 Mass Scaling

Mass scaling tool and its mechanism was discussed previously and it was mentioned that this tool has great effect on reducing the total simulation time. It was also noted that the amount of mass scaling factor should be reasonable in order to make the results acceptable. The only way to find out whether a specific amount of mass scaling will work for the simulation or not is trial and error. On table 4.7 the list of mass scaling amounts used for different stages of the process are shown.

Table 4.7: The mass scaling factors that were used for different stages of FEA.

| Number of stage and degree | Mass scaling factor |
|---|---|
| 1st 45 degree | 25 |
| 2nd 60 degree | 25 |
| 3rd 75 degree | 16 |
| 4th 90 degree | 4 |

Of course all of these mass scaling factors are below the limit line. For example for the 45°stage the upper limit for MSF (mass scaling factor) is 64, but as seen in the table MSF of 25 is used. Or for the 90°stage MSF upper limit is 16. But the point is this upper limit is valid until only 90°stage is running and there will be no other 3

stages. In real simulation all 4 stages are active so the material goes under work hardening because of that the whole MSF are lowered to avoid distortion of the elements and maintain the process within the reasonable limits. Mass scaling factor is greatly influenced by work hardening. Using any mass scaling factor under the upper limit will have no effect on the results of the simulation [30].

### 4.3.5 Element Selection Method for Comparison

In order to study different aspects of FEA results, a series of elements are chosen. In this section how these elements are selected and what type of limitations we have will be explained.

There will be two types of element selection in this study. The first one is selecting a row of elements in a single part. In order to do that a line of elements along the depth of the sheet are selected like shown in figure 4.18.

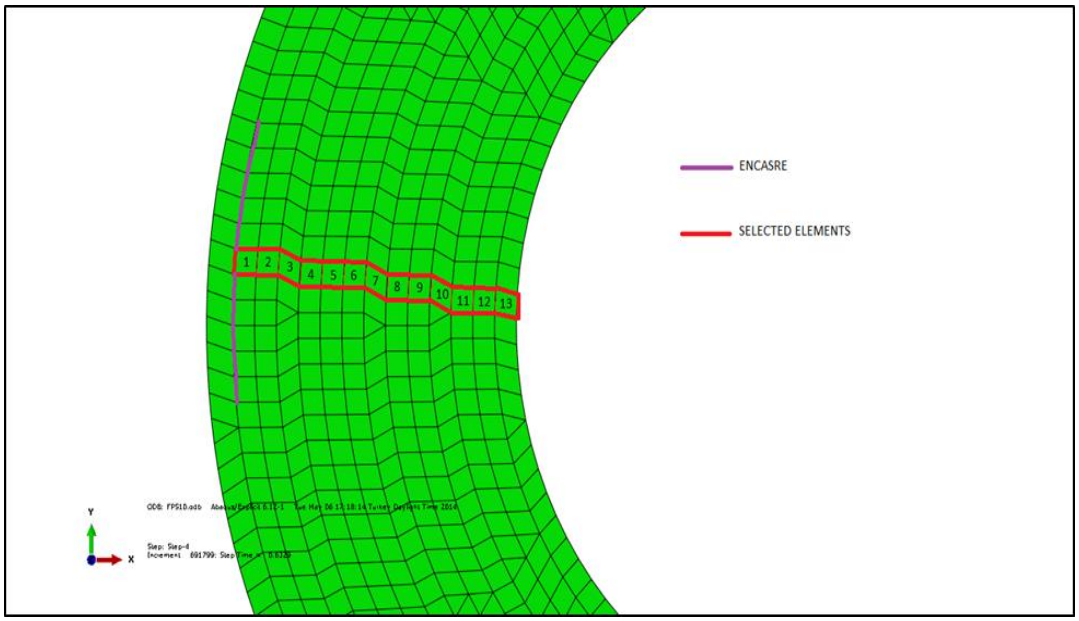


Figure 4.18: Selection of the study candidate elements in ABAQUS.

The elements are not aligned on a straight line which were not available too. Also the 80mm holed part is shown in the figure and as the hole size gets bigger some common elements will be lost. For example in the 95mm holed part only seven elements are common among all parts and can be studied. All of the selected elements are quad ones and all the tri elements were avoided to increase the accuracy of the comparison.

# Chapter 5

# RESULTS AND DISCUSSION

In this chapter the results of changing hole size on different parameters of hole flanging will be discussed. 5 hole sizes were selected as follows:

75, 80, 85, 90, and 95 mm

The preselected parameters in order to make the parts with experiments were discussed before and also the same situation is valid for the FEA simulation too.

## 5.1 Total Depth Or Formability

Despite the fact that in the CNC program all the stages were set to 35 mm depth, whenever the failure occurred the test were stopped. So the total depth achieved without failure were investigated. The results for total depth achieved in the experiments are in figure 5.1.

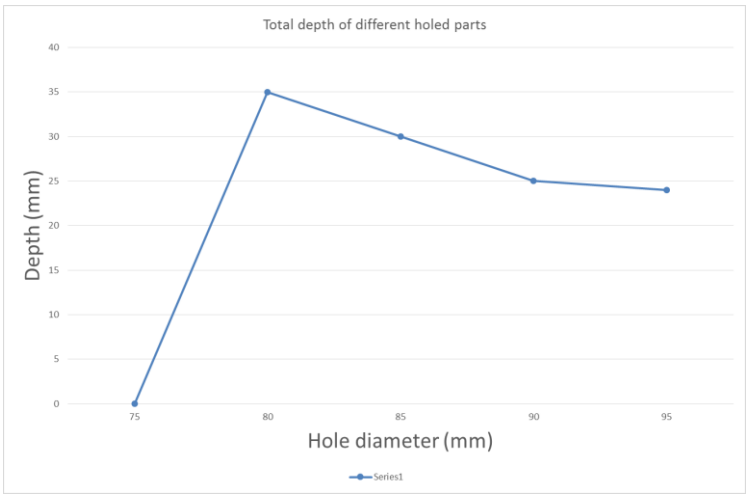


Figure 5.1: Total depth without failure achieved for parts via tests.

It is important to mention that the part with 75mm hole size didn't reach the 4$^{th}$ stage

and failed in the 3rd one. So the depth for that part is considered zero. From the chart above it is obvious that the total depth with increasing amount of hole size decreases. Maximum depth is reached in 80mm hole size part. It can be assumed that for this condition of material and experimental set up none of the parts with hole size below 80 mm can reach to 4th stage due to increased stress levels that will be discussed later. Considering that the failure occurred in 80mm hole size at the depth of 35mm, failure occurred in 85mm in depth of 30 and 90 and 95mm parts were without failure, we can claim that increasing the hole size has a great effect in reducing the overall stress state preventing the part to fail. Another notable point is as the hole gets bigger the total amount of material that is going to be deformed reduces. We lose some material and that means there will be less material to be deformed leading to decreased formability. This can explain despite the fact that the stress level in the 90 or 95mm holed part is lower but the overall depth reached in this level is lower than 80mm holed part.

Figure 5.2: 95 mm holed part – No failure occurred.

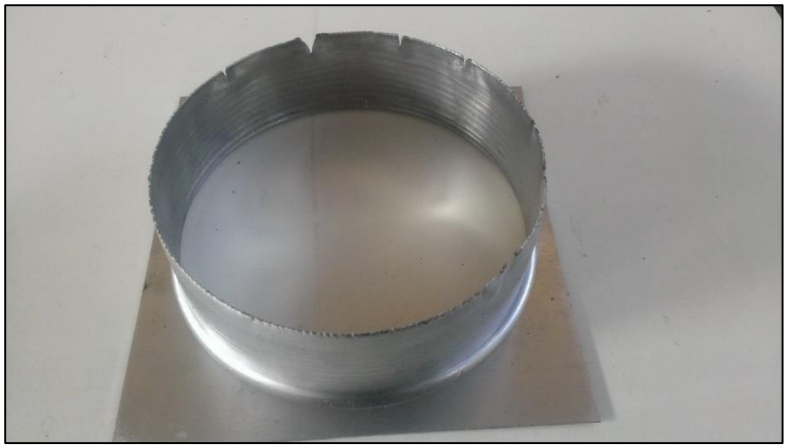

Figure 5.3: 80 mm holed part – Major failure occurred at the edges.

## 5.2 Thickness Distribution

Movement of the tool on the sheet causes the material to flow across the part, from top to bottom [28]. This will make the thickness of the sheet different in each point. Thickness distribution is important due to study where the thinning occurs which is one of the major phenomena's happening during incremental forming.

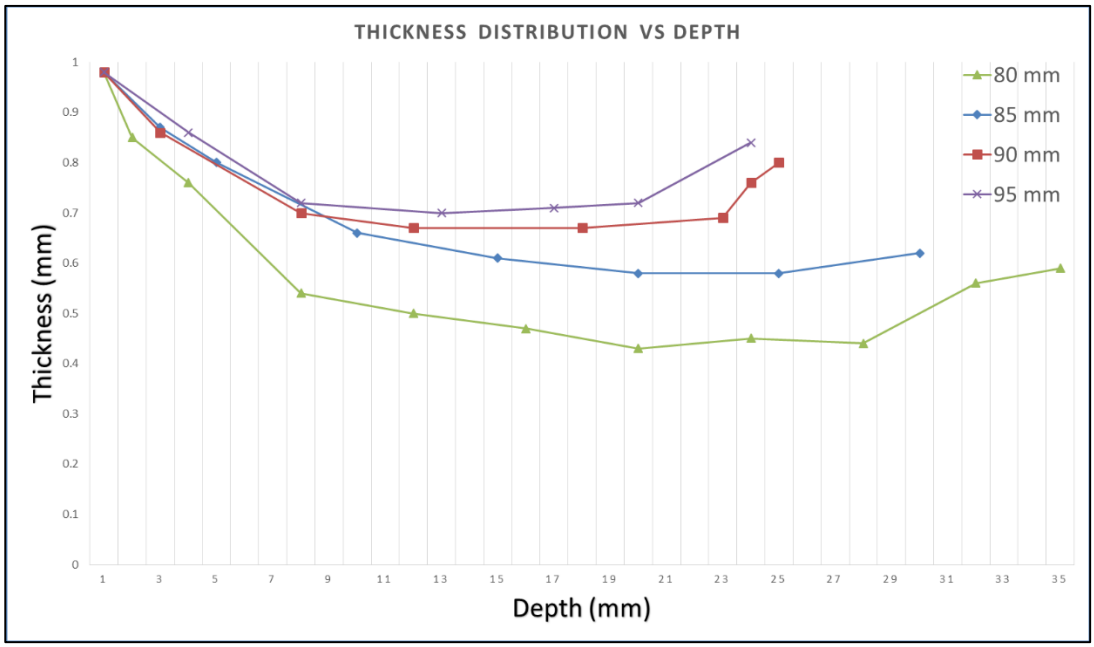


Figure 5.4: Thickness distribution of 80, 85, 90 and 95 mm holed parts.

The thickness distribution for 4 parts are shown in figure 5.4. As seen the minimum wall thickness belongs to part with hole diameter 80mm which had the maximum depth too. It is obvious that as the hole size increases the overall thickness of the wall increases. This means that it prevents thinning and also it increases the minimum wall thickness. It is very interesting that the region with minimum thickness among the parts are almost the same and in the middle of the part.

The parts made by CNC machine are shown in the pictures below. As said the part with 75mm hole size didn't reach the $4^{th}$ stage. The 80mm holed part fails in the depth of 35mm and the 85mm holed part fails in 30 mm depth. The other parts didn't fail till the end of the process.

Figure 5.5: 90 mm holed part – No failure occurred.

It is obvious that despite the fact that with increasing the hole size the failure of the material delays or no failure occurs at all, but the total depth of the parts decreases. Depth, being as a formability factor reduces with increasing the hole size. The FEA results may help to understand the reason why this happens.

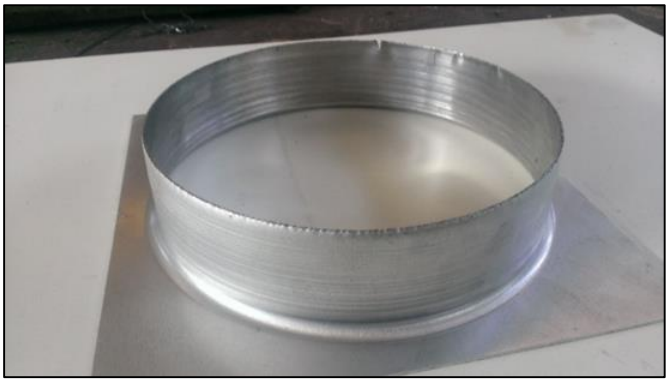

Figure 5.6: 85 mm holed part – Minor failure occurred at the edges.

## 5.3 FEA Results

### 5.3.1 Stress Evolution

Because the material is continuously undergoes load and unload the work hardening is very important here. As the part gets work hardened it requires more stress to be deformed and the overall stress level will increase. In order to compare the stress levels it is important to note that due to work hardening of the material the last stage is the most significant stage of the process. All the failures occurs in that stage and the material is in the highest work hardened level. Also the ending edges of the element selection are the most important elements due to failing. The last stress level for all ending elements of the parts are listed table 5.1.

Table 5.1: Maximum v.Misses stress achieved for different hole sizes in FEA. The last element of the edges were selected.

| Hole size (mm) | v.Misses Stress ($\times 10^2$ MP) |
|---|---|
| 75 | 4.52 |
| 80 | 3.93 |
| 85 | 3.12 |
| 90 | 3.75 |
| 95 | 3.50 |

It is obvious that the highest stress level is reached in the part with 75mm hole diameter which didn't reach the 4$^{th}$ stage. And also let me mention that the stress level for 75mm holed part was 4.52 $\times 10^2$ MP which was very close to $4.84 \times 10^2$ MP the UTS point of the material. Increasing the hole size to 80 mm the stress level reduces to $3.93 \times 10^2$ MPa So the pattern shows that after the 75mm hole size the role of hole gets significant, greatly decreasing the maximum stress level of the parts and delaying the failure.

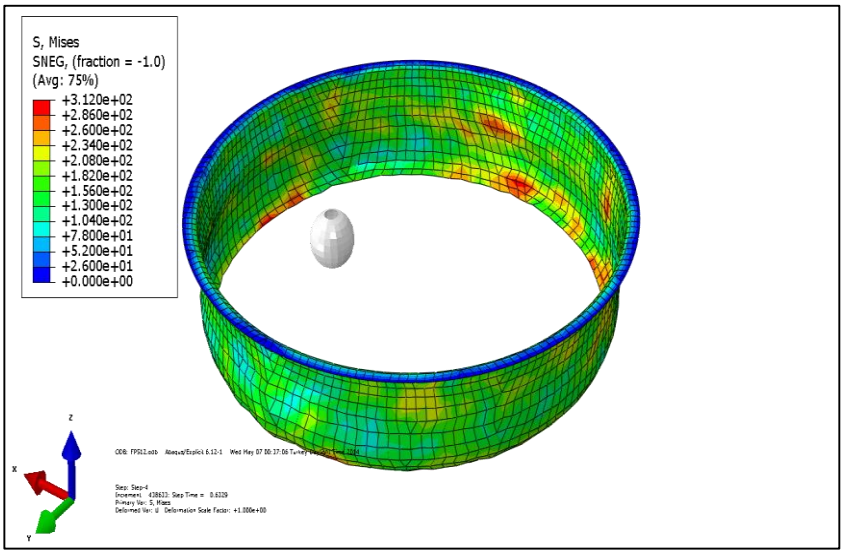

Figure 5.7: 85 mm holed part – Misses stress distribution (MPa).

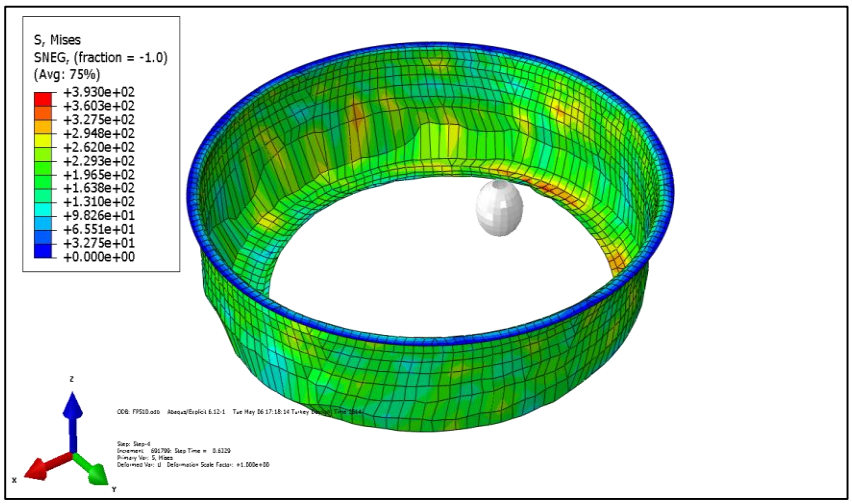

Figure 5.8: 80 mm holed part – Misses stress distribution (MPa).

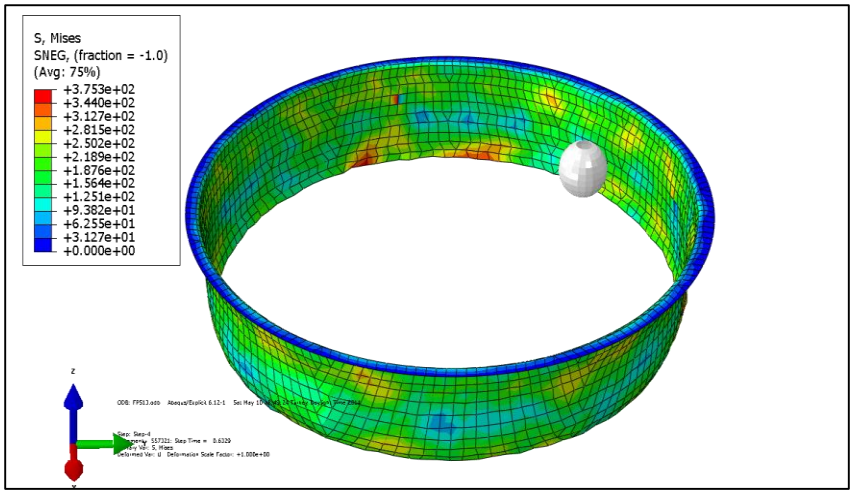


Figure 5.9: 90 mm holed part – Misses stress distribution (MPa).

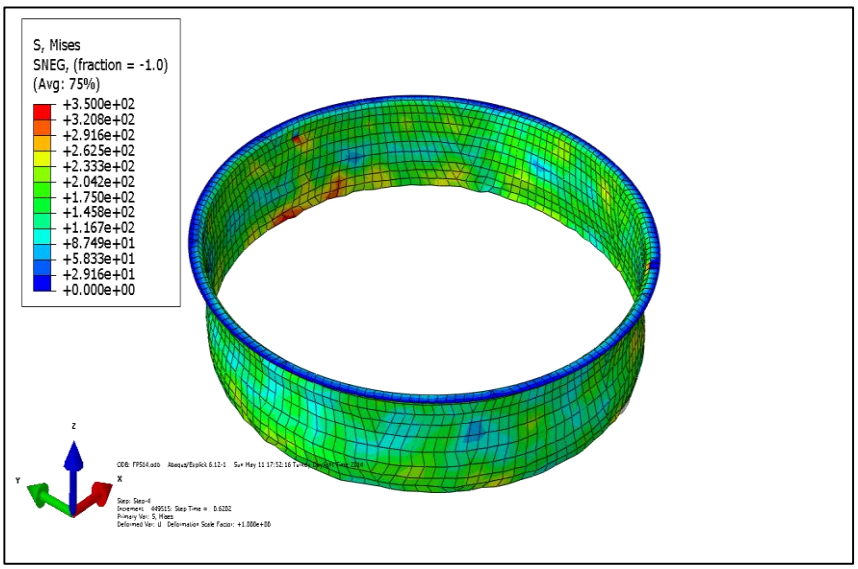


Figure 5.10: 95 mm holed part – Misses stress distribution (MPa).

The stress evolution graph with respect to time for 2 common elements are shown below. The first one is element number 1 and the second is element number 7 (see Figure 4.7) that are common among all the parts.

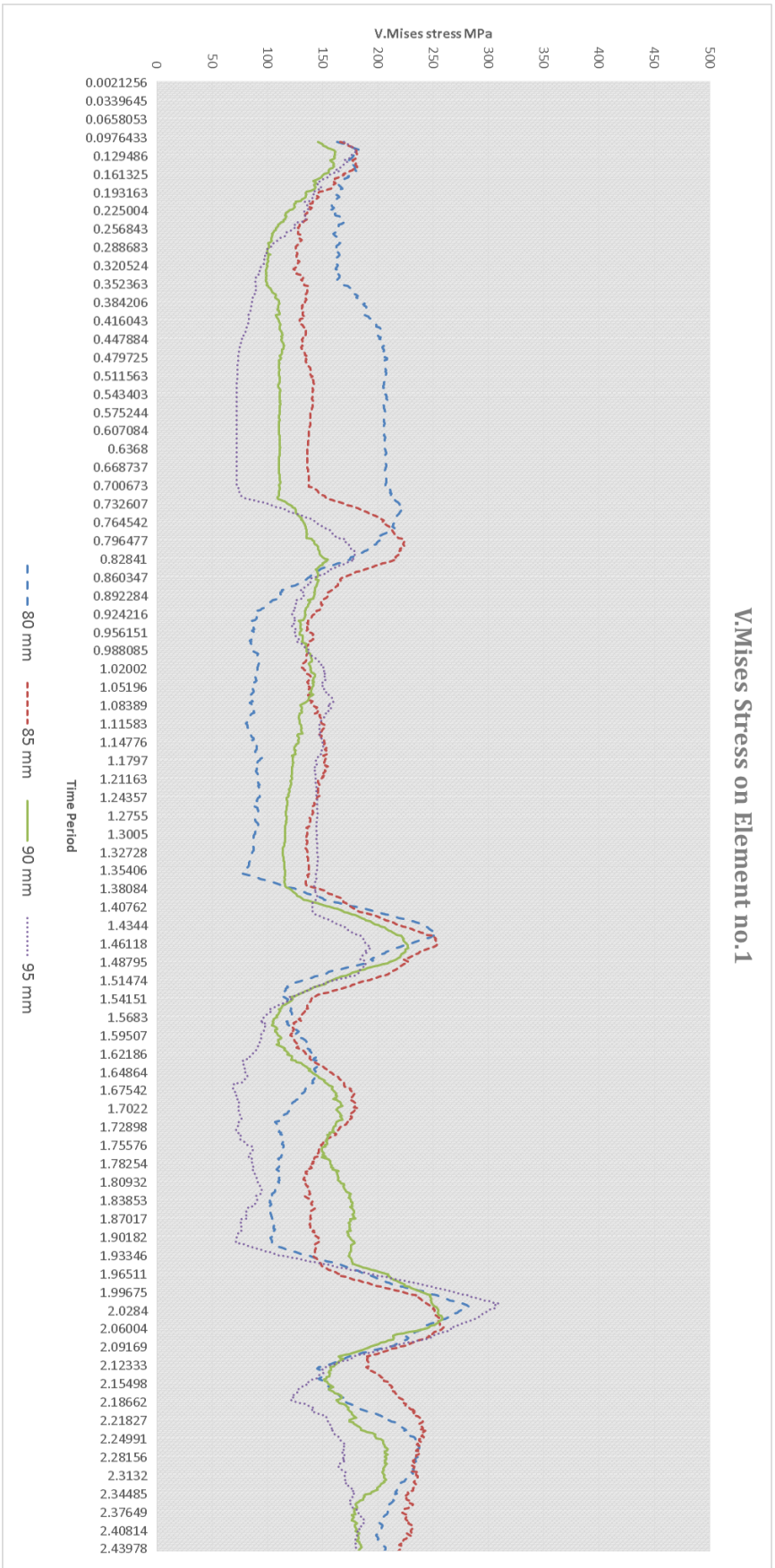


Figure 5.11: Misses stress evolution for element num. 1 in different holed parts.

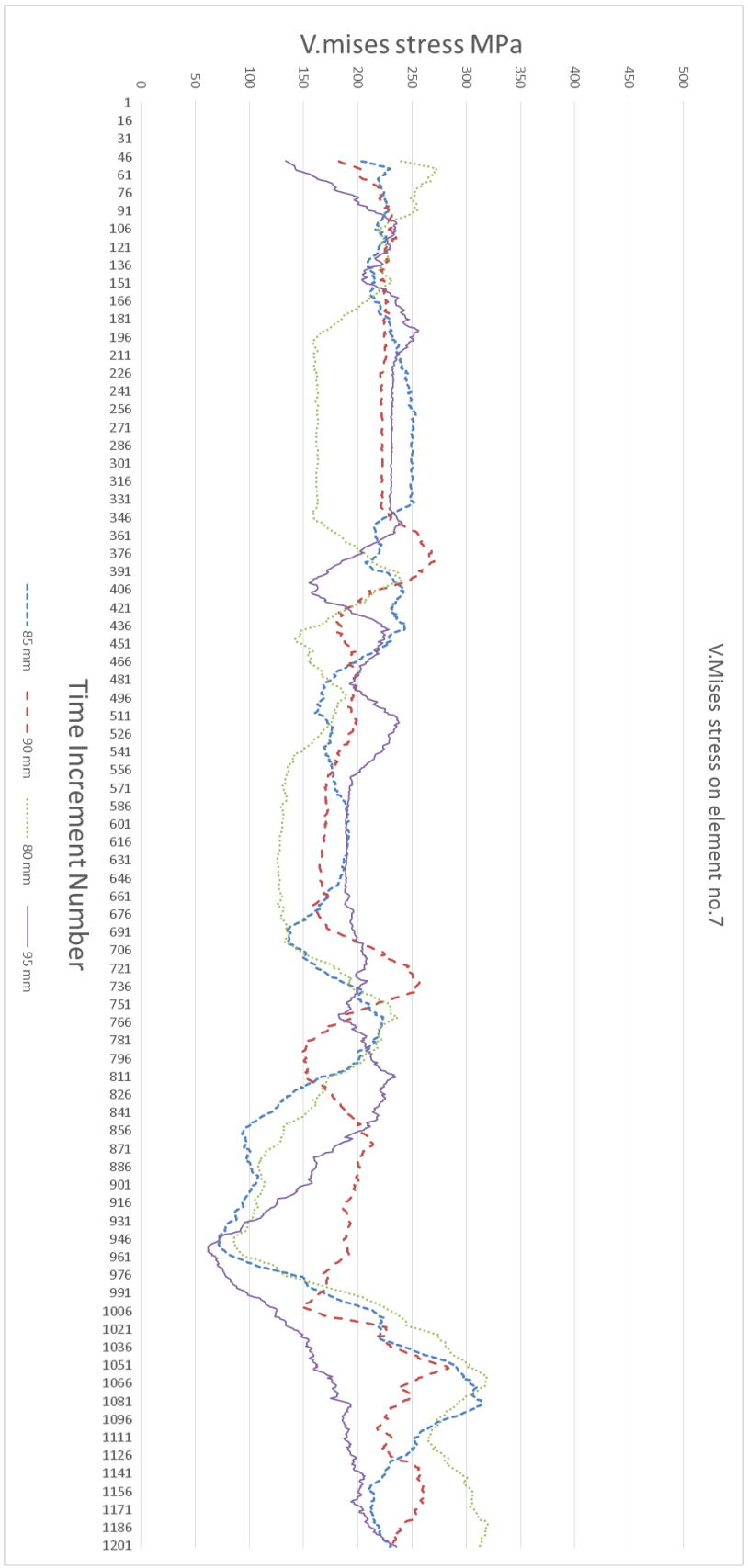


Figure 5.12: v.Misses stress evolution for element num. 7 in different holed parts except the part with 75mm hole diameter.

In the figure 5.11 every 0.63 seconds is a stage. It is notable that despite the fact that the part with 80mm hole diameter has the highest stress level in the first stage but in the significant 4$^{th}$ stage the maximum stress belongs to 95mm holed part. Now let's take a look at the 7$^{th}$ element's stress vs time graph.

In the last element in the significant 4$^{th}$ stage the maximum stress belongs to 80 and 85mm holed parts. This pattern is valid for almost all of the elements and proves that the part with 80mm hole diameter critical last element owns the most stress levels among all others. With considering the work hardening issue it can be claimed that the higher stress and work hardening in a reasonable level will lead to higher formability. If the stress gets too high like what we had in part with 75mm hole diameter the failure will occur earlier and if the stress level is too low the material will not fail but the formability will be decreased corresponding to the stress level. That is why the highest formability is achieved in part with 80mm hole size which is in a good agreement with the experiments results. The stress levels for part with 80mm hole size in ABAQUS are shown in figure 5.13.

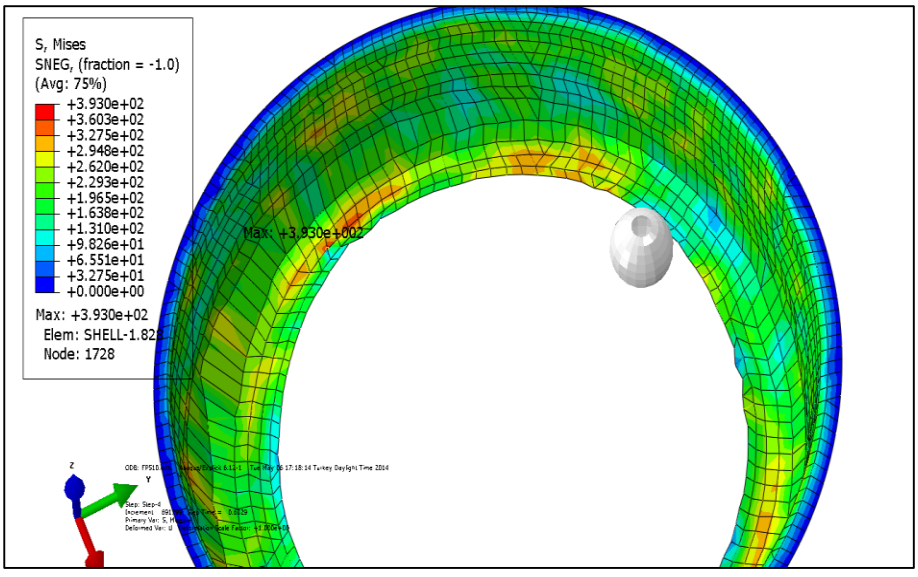

Figure 5.13: 80 mm holed part – maximum stress element is highlighted.

The maximum stress occurs in the element colored in red. Let's take a look at the 80mm holed part. The same element in the actual part is the first element that starts failing. This shows the good agreement between the simulation and experiments.

### 5.3.2 Strain Evolution

The thickness distribution among the parts were studied in the experiments results section. Let's take a look at figure 5.4 again.

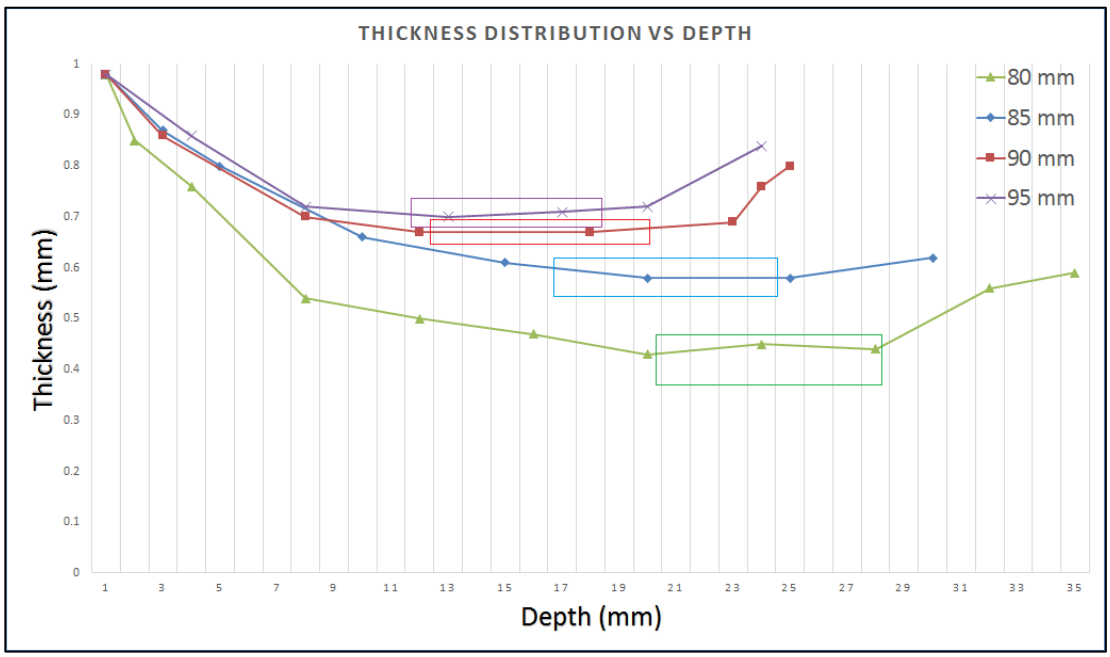


Figure 5.4: Thickness distribution of 80, 85 and 90 mm holed parts. Thinning areas are high lightened.

The region where minimum thickness or thinning occurs is high lightened. This region is almost in the middle of all parts and almost common among all of them. This region ends when we are entering the critical edges where the failure usually happens and the material flow is towards it [28] so the thickness will increase significantly after this region. The diagram also shows that as the hole size gets bigger thinning effect reduces this means that the difference between the thickest area in the last point of edges and

the thinnest area in the middle region decreases so lowering the material flow in the part.

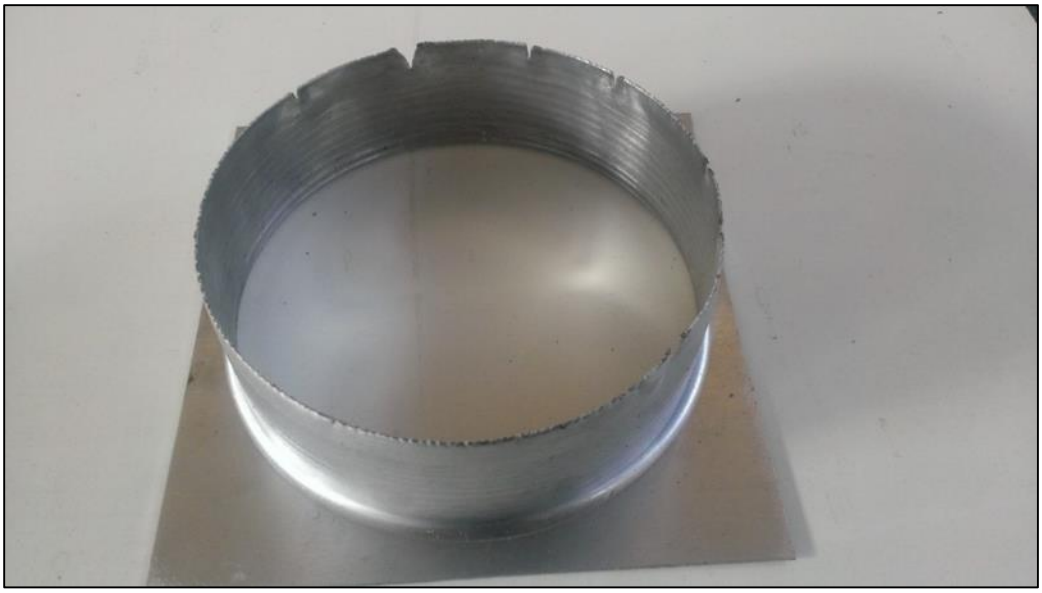

Figure 5.14: 80 mm holed part and the failure points at the edges.

Now let's see what happens in this region in the FEA simulation. The maximum and minimum in-plane strain of part with 85mm hole size are shown in figure 5.15 and 5.16.

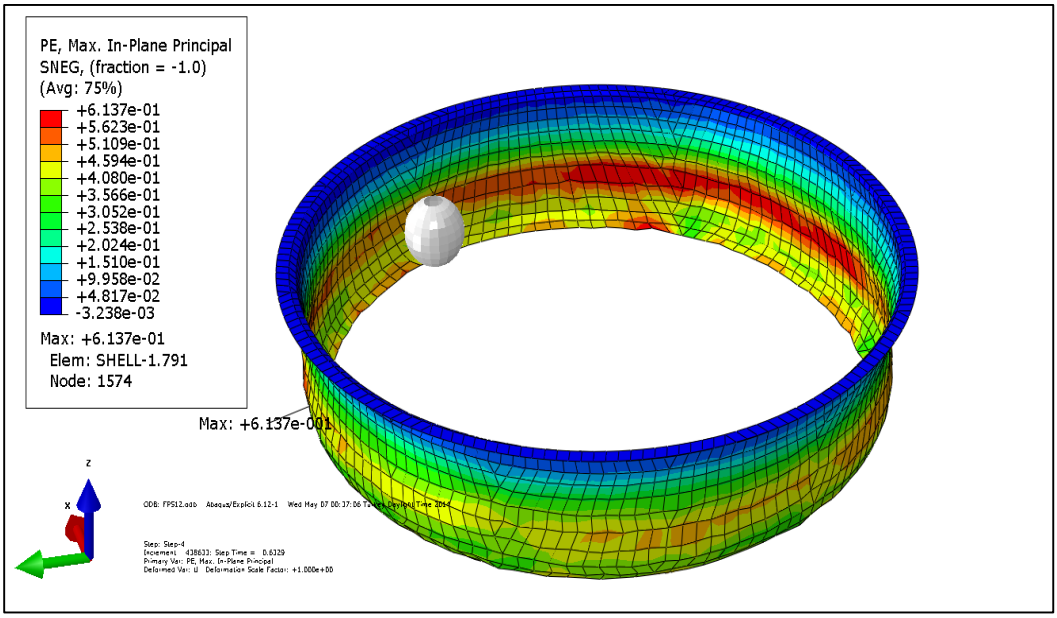

Figure 5.15: 85 mm holed part - Maximum in-plane strain (mm).

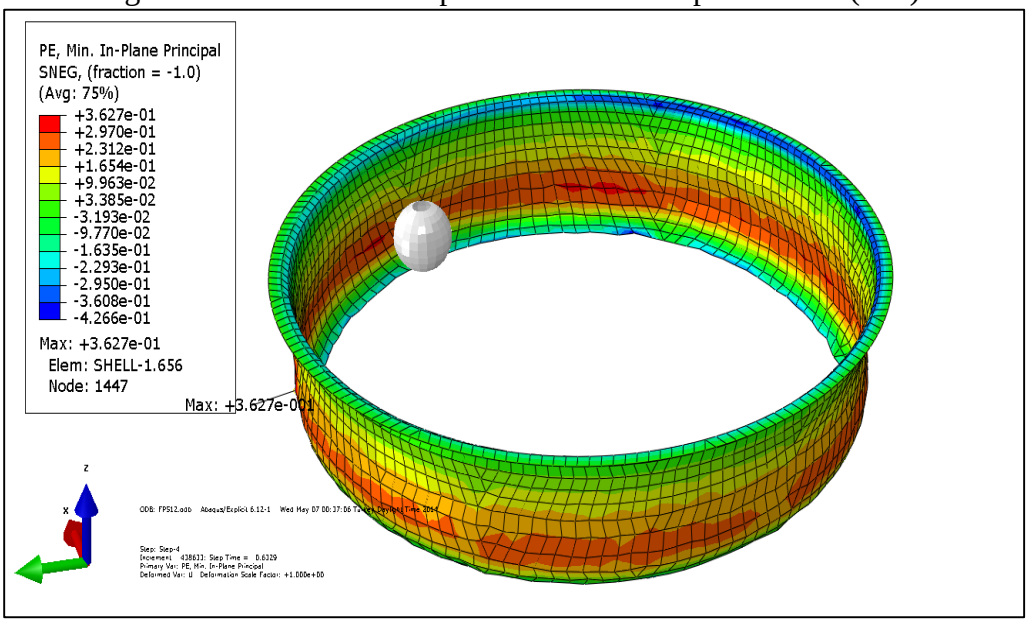


Figure 5.16: 85 mm holed part - Minimum in-plane strain (mm).

The pictures show that the max and min in-plane strain occurs in the same region and also shows that the part undergoes to biaxial strain in this region. This biaxial strain will lead to higher material flow from this region and causes to make the region thinner the same as what we had in the experiments results and is in a good agreement with the experimental results.

Let's consider the holed part 80 mm and 75 mm which didn't make it to 4$^{th}$ stage and failed before that. First of all the stress level of part with 80mm hole size is less than the other one. Second, in part with 75mm hole size there is much more material under the tool which is going to be deformed. This much material under the tool bends under it and causes the tool to flow the material in 2 plane directions. In other words:

$\varepsilon_{1\neq0}$ And $\varepsilon_{2\neq0}$ Eq.5.1

These 2 strains are called longitudinal and hoop strains respectively. When the hole size gets bigger the amount of material under load by tool decreases. This means that there is less material to be deformed in the direction of tool movement that defines hoop strain.

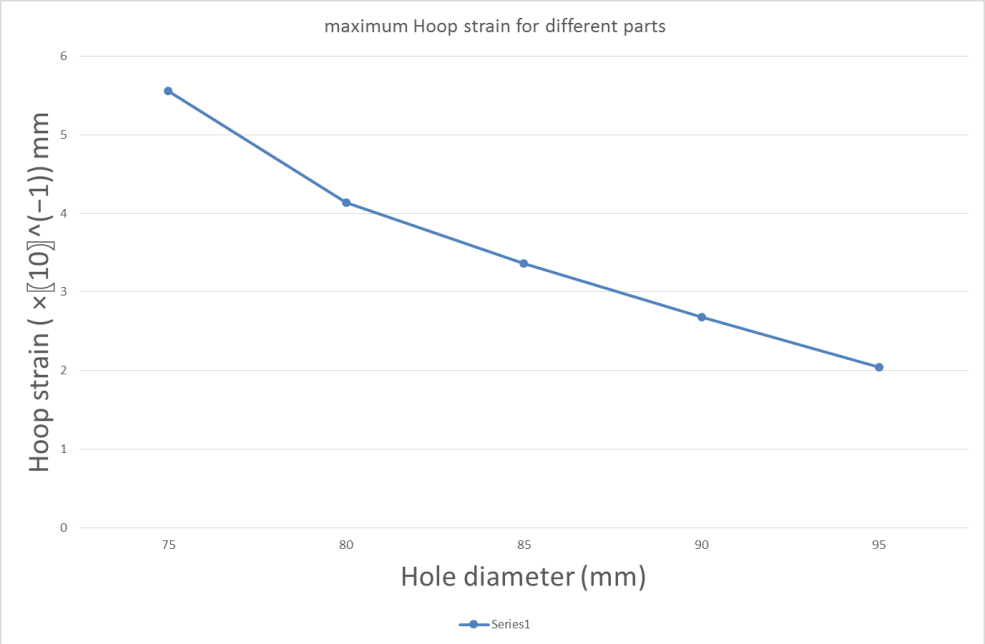

Figure 5.17: Maximum hoop strain (mm) for different holed parts element no 7.

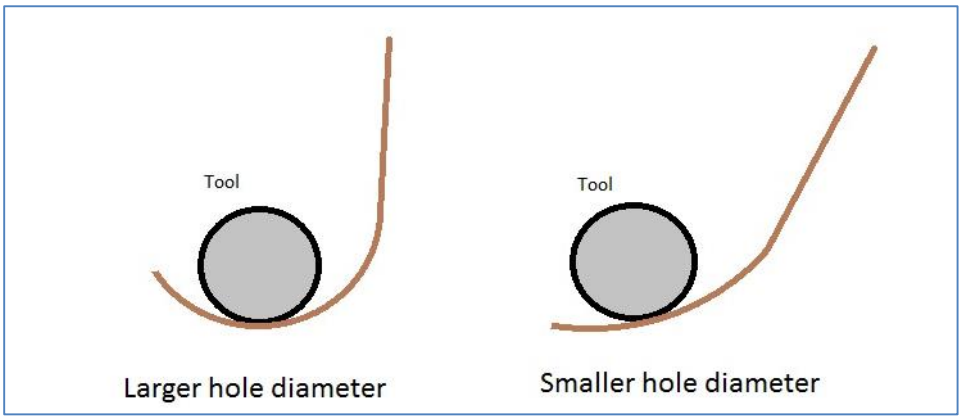

Figure 5.18: Tool approach encountering smaller or larger hole diameter.

Now in the part with 80mm hole size the material under load in comparison with 75 mm is less, so the hoop strain is less too. Maybe this reduction in hoop strain caused

by bigger hole size is connected to stress levels. So up to now we know that that bigger hole size means smaller hoop strain. If we consider the volume constancy law:

$$\boldsymbol{\varepsilon}_1 + \boldsymbol{\varepsilon}_2 + \boldsymbol{\varepsilon}_3 = 0 \qquad \text{Eq. 5.2}$$

In the matter of part with 80mm hole size the hoop strain is less than the 75 mm. in the matter of longitude strain we have almost the same amount. This means thickness strain in the matter of 75 mm should be bigger than 80 mm which is also true. Thinning was almost that intense in 75 mm that caused failure before reaching 4$^{th}$ stage. This strain behavior can be studied from another point of view. When the hole size is smaller the increased material under tool causes rise in contact area. Increasing contact area will provide more material under tool to be deformed in the direction of tool movement and increasing the hoop strain.

As we go further and increase the hole size we reach part with 85mm hole size which has lower stress level than 80 mm. higher stress level of 80 mm shows that a reasonable amount of work hardening is useful to increase the formability of this process. And of course further increase will provide more stress level and more work hardening level which will cause early failure like we had in 75 mm holed part. As we increase the hole size to 90 and 95 mm the stress level increases due to FEA results. It is expected that failure will occur due to increase in stress level but that never happened. The reason of this may lay on the fact that increased hole size reduces the material amount that is going under load and due to lack of material.

# Chapter 6

# CONCLUSION AND FUTURE WORKS

1. In the current study the effect of the hole size on formability of hole flanging by multistage incremental forming was investigated. The selected hole diameters are 75, 80, 85, 90 and 95 mm and also the aluminum sheet is in square shape with length of 142 mm with thickness of 1 mm. It has been found that increasing the hole diameter will prevent early failure leading to higher formability until the part with 80mm hole size and further increase will lead to decreased formability due to lack of material. The maximum formability was reached in part with 80mm hole diameter.
2. The results show that larger hole diameter will increase the thickness of the thinning area and also the final thickness of the edges due to reducing the material under load by the tool and in turn decreased hoop strain.
3. The FEA results showed that increasing the hole size will decrease the stress levels and preventing failure, Also lowering the work hardening level. Despite the fact that increasing the hole size will provide lower stress levels but in case of part with 80mm hole diameter higher stress led to higher formability and proved that a reasonable amount of stress and work hardening level is useful to increase the formability of the process.
4. The FEA results showed that the max and min in-plane strains occurs in the same region, so the deformation there is biaxial. That's exactly the region with lowest thickness (thinning area). That proves the significance of hoop strain

where lowered the thickness of that region dramatically in all the parts. But it was shown that as the hole diameter gets bigger, the hoop strain decreases so the thinning area will have more thickness like what we observed in 90 and 95 mm holed parts.

5. The maximum formability were reached in part with 80mm hole diameter due to a sufficient amount of stress and work hardening level. The applicability of this finding needs to be investigated for other materials also.
6. The maximum formability were achieved with limiting forming ratio (see section 2.4.1.1) of 1.775. The size of hole diameter and part diameter should be varied to investigate the generality of this value.

# REFERENCES

[1] T. Schafer , R.D. Schraft, Incremental sheet metal forming by industrial robots using a hammering tool, 10emes Assises Europeennes de Prototypage Rapide, Paris, France (2004).

[2] E. Hagan and J. Jeswiet, A review of conventional and modern single point sheet metal forming methods. Journal of Engineering Manufacture, 217 (2003) 213-225.

[3] Ham and J. Jeswiet, Single Point Incremental Forming and the Forming Criteria for AA3003, Mechanical & Materials Engineering, Queen's University, Kingston, ON, Canada.

[4] Fratini, L., Ambrogio, G The influence of mechanical properties of the sheet material on formability in single point incremental forming.

[5] Martins, P.A.F. Bay, N. Skjoedt, M. Silva, M.B. Theory of single point incremental forming. Journal of Strain Analysis. 43(2008), 15-35.

[6] R. Joost Duflou, Joris Dhondt, Applying TRIZ for systematic manufacturing process innovation: The single point incremental forming case, Procedia Engineering 9 (2011), pages 528-537.

[7] Flores, P. Duchene, L. Bouffioux, C. Lelotte, T. Henrard, C. Pernin, N. Van Bael, A. He, S. Duflou, J. Habraken, A.M. Model identification and FE simulations: Effect of different yield loci and hardening laws in sheet forming. International Journal of Plasticity, 23 (2007), 420-449.

[8] M. Ham, J. Jeswiet, Single point incremental forming and the forming criteria 2011.

[9] Isekia, H. Naganawab, Vertical wall surface forming of rectangular shell using multistage incremental forming with spherical and cylindrical rollers. Journal of Materials Processing Technology. 130(2002), 675–679.

[10] J. Jeswiet, F. Micari, G. Hirt, A. Bramley, J. Duflou, J. Allwood, Asymmetric single point incremental forming of sheet metal, CIRP Annals, 54(2005), 623-650.

[11] Isekia, H. Naganawab, Vertical wall surface forming of rectangular shell using multistage incremental forming with spherical and cylindrical rollers. Journal of Materials Processing Technology. 130(2002), 675–679.

[12] Duflou, J.R Callebaut, B. Verbert, J. De Baerdemaeker, H. Laser Assisted Incremental Forming: Formability and Accuracy Improvement. CIRP Annals, 56(2007),273-276.

[13] J. Jeswieta, F. Micarib, G. Hirtc, A. Bramleyc, J. Dufloue, J. Allwoodf CIRP Asymmetric Single Point Incremental Forming of Sheet Metal Annals - Manufacturing Technology
Volume 54, Issue 2, 2005, Pages 88–114

[14] F. Micari, M. Geiger, J. Duflou, B. Shirvani, R. Clarke, R. Di Lorenzo and L. Fratini Two Point Incremental Forming with Two Moving Forming Tools July, 2007

[15] M.B. Silva, P. A. F. Martins Journal of Materials Engineering and Performance April 2013, Volume 22, Issue 4, pp 1018-1027
Two-Point Incremental Forming with Partial Die: Theory and Experimentation.

[16] http://cao.mech.northwestern.edu/incremental_forming.html

[17] D. Young and J. Jeswiet. Forming Limit Diagrams for Single-Point Incremental Forming of Aluminium Sheet. In Proc. of the IMechE, Journal of Engineering Manufacture - Part B, vol. 219, pp. 359364, 2005. doi:10.1243/095440505X32210.

[18] W. C. Emmens and A. H. van den Boogaard. Tensile tests with bending: a mechanism for incremental forming. International Journal of Material Forming (2008). doi:10.1007/s12289-008-0185-y.

[19] A. Van Bael, P. Eyckens, S. He, P. Van Houtte, C. Bouffioux, C. Henrard, A. M. Habraken, and J. R. Duflou. Forming Limit Predictions For Single-Point Incremental Sheet Metal Forming. In Proc. of the 10th Esaform conference, vol. 907 of AIP Conf. Proc., pp. 309314, 2007. doi:10.1063/1.2729530.

[20] P. Flores, L. Duchêne, T. Lelotte, C. Bouffioux, F. El Houdaigui, A. Van Bael, S. He, J. R. Duflou, and A. M. Habraken. Model Identication and FE Simulations: Eject of Different Yield Loci and Hardening Laws. In L. M. Smith, F. Pourboghrat, J.-W. Yoon, and T. B. Stoughton, editors, Proc. of the 6th Numisheet Conference, vol. 778, pp. 3714381, Detroit, MI, USA, 2005. AIP Conf. Proc. doi:10.1063/1.2011248.

[21] W. C. Emmens and A. H. van den Boogaard. Strain in Shear, and Material Behaviour in Incremental Forming. Key Engineering Materials 344 (2007), pp. 519526.

[22] A. Van Bael, P. Eyckens, S. He, Forming Limit Predictions for the Serrated Strain Paths in Single Point Incremental Sheet Forming. In Proc. of the 9th Numiform

[23] W. C. Emmens and A. H. van den Boogaard. Incremental Forming Studied by Tensile Tests with Bending. In Proc. of the 9th ICTP conference, pp. 508513, Gyeongju, Korea, 2008. Tue Korean Society for Technology of Plasticity.

[24] P. A. F. Martins, N. Bay, M. Skjoedt, and M. B. Silva. Theory of single point incremental forming. CIRP Annals Manufacturing Technology 57, 1 (2008), pp. 247252. doi:

[25] J.R. Duflou, J. Verbert, B. Belkassem , J. Gub, H. Sol, C. Henrard, A.M. Habraken, Process window enhancement for single point incremental forming through multi-step tool paths CIRP Annals - Manufacturing Technology 57 (2008) 253-256.

[26] J. R. Duflou, J. Verbert, B. Belkassem, J. Gu, H. Sol, C. Henrard, and A. M. Habraken. Process Window Enhancement for Single Point Incremental Forming through Multi-Step Toolpaths. CIRP Annals Manufacturing Technology 57 (2008), pp. 253256. doi:10.1016/j.cirp.2008.03.030.

[27] G. Centeno a, M.B.Silva b, V.A.M.Cristino b, C.Vallellano a, P.A.F.Martin. Hole-flanging by incremental sheet forming.

[28] Z. Cui , L. Gao, Studies on hole-flanging process using multistage incremental forming, a College of Mechanical and Electrical Engineering, Nanjing University of Aeronautics and Astronautics, Nanjing 210016, PR China College of Engineering, University of Michigan, Ann Arbor 48109-2125.

[29] K.-J. Bathe and E. L. Wilson. Numerical Methods in Finite Element Analysis. PrenticeHall, Inc., Englewood Clis, New Jersey, 1976.

[30] ABAQUS Manual.

[31] G. Ambrogio, L. Filice, F. Gagliardi, and F. Micari. Sheet Thinning Prediction in Single Point Incremental Forming. Advanced Materials Research 68 (2005), pp. 479486.

[32] M. Bambach and G. Hirt. Performance Assessment of Element Formulations and Constitutive Laws for the Simulation of Incremental Sheet Forming(ISF). In E. Oñate and D. R. J. Owen, editors, Proc. of the 8th Complas conference, Barcelona, 2005. CIMNE.

[33] S. He, A. Van Bael, P. Van Houtte, A. Szekeres, J. R. Duflou, C. Henrard, and A. M. Habraken. Finite Element Modeling of Incremental Forming of Aluminum Sheets. Advanced Materials Research 6-8 (2005), pp. 525532.

[34] C. Bouffioux, C. Henrard, P. Eyckens, R. Aerens, A. Van Bael, H. Sol, J. R. Duflou, and A. M. Habraken. Comparison of the Tests Chosen for Material Parameters Identification.

[35] J. Mackerle, Finite element analyses and simulations of sheet metal forming processes. Engineering Computations, 21 (2004) 891-940.

[36] MB Silva, P Teixeira, A Reis and PAF Martins, Proceedings of the Institution of Mechanical Engineers, Part L: Journal of Materials Design and

Applications 2013 227: 91 On the formability of hole-flanging by incremental sheet forming.

[37] H. Iseki, Journal of Materials Processing Technology Volume 111, Issues 1–3, 25 April 2001, Pages 150–154 International symposium on advanced forming and die manufacturing technology.

[38] Hagan, E., Jeswiet, J. Analysis of surface roughness for parts formed by computer numerical controlled incremental forming. Proc. IMechE. J. Engineering Manufacture. (2004).